Seismotectonics in Northeastern France and neighboring regions

Cécile Doubre, Mustapha Meghraoui, Frédéric Masson, Sophie Lambotte, Hélène Jund, Maxime Bès de Berc, Marc Grunberg

INSTITUT DE FRANCE
Académie des sciences

Comptes Rendus

Géoscience

Sciences de la Planète

Cécile Doubre, Mustapha Meghraoui, Frédéric Masson, Sophie Lambotte, Hélène Jund, Maxime Bès de Berc and Marc Grunberg

Seismotectonics in Northeastern France and neighboring regions

Online first, 8th September 2021

<https://doi.org/10.5802/crgeos.80>

Part of the Special Issue: Seismicity in France

Guest editors: Carole Petit (Université de Nice, CNRS, France), Stéphane Mazzotti (Université Montpellier 2, France) and Frédéric Masson (Université de Strasbourg, CNRS, France)

Les Comptes Rendus. Géoscience — Sciences de la Planète *sont membres du Centre Mersenne pour l'édition scientifique ouverte*
www.centre-mersenne.org

Comptes Rendus
Géoscience — Sciences de la Planète
Online first, 8th September 2021
https://doi.org/10.5802/crgeos.80

Seismicity in France / *Sismicité en France*

Seismotectonics in Northeastern France and neighboring regions

Cécile Doubre [a]*, Mustapha Meghraoui [a], Frédéric Masson [a], Sophie Lambotte [a], Hélène Jund [b], Maxime Bès de Berc [a] and Marc Grunberg [b]

[a] ITES, Université de Strasbourg, CNRS, ENGEES, Institut Terre et Environnement de Strasbourg, UMR 7063, 5 rue Descartes, Strasbourg F-67084, France

[b] EOST, Université de Strasbourg, CNRS, Ecole et Observatoire des Sciences de la Terre, UMS 830, 5 rue Descartes, Strasbourg F-67084, France

E-mails: cecile.doubre@unistra.fr (C. Doubre), mustapha.meghraoui@unistra.fr (M. Meghraoui), frederic.masson@unistra.fr (F. Masson), sophie.lambotte@unistra.fr (S. Lambotte), helene.jund@unistra.fr (H. Jund), maxime.besdeberc@unistra.fr (M. Bès de Berc), marc.grunberg@unistra.fr (M. Grunberg)

Abstract. The region of northeastern France is affected by low-magnitude background seismicity, with the rare occurrence of moderate earthquakes, which gives this region a non-negligible seismic risk. We provide an overview of the seismicity and seismotectonics of this intraplate domain and of its sub-regions: the Upper-Rhine Graben (URG), the external range and foreland of Jura, the Vosges, northern France and southern Belgium. Previously published catalogues over historical and instrumental times are used, and the epicentral distribution of earthquakes is compared to known tectonic structures, and the recently computed deformation field. Although no large earthquakes with $M_W > 6.0$ occurred since the 1356 Basel seismic event (Io IX, MKS), the recent identification of active faults suggests periods of high seismic strain rates in the past. The origin of the seismic activity in each of these sub-regions, characterized by low to very-low strain rates, is attributed to pre-existing faults reactivated under specific natural or anthropogenic conditions.

Keywords. Seismicity, Active fault, Northeastern France, Intraplate domain, Low strain region.
Online first, 8th September 2021

1. Introduction

Northwestern Europe is considered as one of the best examples for intraplate seismicity. The occurrence of several earthquakes in western Europe with a moderate magnitude made its mark on the population and the cities during both the historical and the instrumental periods. With a maximum intensity of IX, the 1356 Basel earthquake (Switzerland and France), for which various magnitudes have been proposed, reaching a maximum value of 7.1, is regularly cited as the strongest earthquake in western Europe [e.g. Mayer-Rosa and Cadiot, 1979, Meghraoui et al., 2001, Ferry et al., 2005, Fäh et al., 2009]. The occurrence of such an event and the regularly recorded microseismicity raises many questions regarding the physical processes involved in the generation of small and large earthquakes in an area of low deformation rate, where the active tectonic structures and their kinematics remain poorly understood. The recent

* Corresponding author.

geodetic analyses in this region based on long time series measurements confirm the low surface displacements and strain rate field [Henrion et al., 2020]. If the seismic energy is released as a sudden slip of locked fault segments in areas of accumulation of elastic deformation due to tectonic forces [Sykes, 1978], it induces a long loading period and large recurrence time (>10,000 years?) between each event as inferred in the Lower-Rhine Graben [Camelbeeck and Meghraoui, 1998]. A damaging earthquake may occur where the seismic hazard was considered low, such as the recent seismic event of Le Teil in France in 2019 [M_w 4.9; Cornou et al., 2021] which struck a region with low background micro-seismicity. As with other seismic events in the intraplate domain, the role of local, anthropogenic or natural, perturbations of the stress state and/or the fault strength have been invoked to explain the occurrence of large intraplate earthquakes [Stein et al., 2015, Calais et al., 2016]. The seismological archives and catalogues combined with the identification of active faults are therefore essential to study the seismic behavior of such a region and better constrain the processes potentially involved in the occurrence of small and large earthquakes.

Micro-seismicity can be seen as an indicator of the seismic potential of a region, pointing out the location of a future moderate/large earthquake. However as underlined by Ebel et al. [2000], the microseismicity and specific sequences of low-magnitude earthquakes in areas of low deformation rates, such as intraplate domains, could also be considered as a sequence of aftershocks of larger seismic events with a return period longer than the period covered by the historical archives [Stein et al., 2015]. Therefore, the absence of knowledge of very old large events makes it difficult to interpret both the current microseismicity and some swarms of events that stand out from the low background regional seismicity as sequences of aftershocks consistent with the Omori law descriptions of seismic rate decrease over time [Omori, 1894, Utsu, 1961]. This low background seismicity is generally diffuse throughout the region and is usually interpreted as due to the presence of a network of numerous small faults likely loaded at various rates, instead of being seen as a large seismogenic structure at crustal or even lithospheric scale along a plate boundary, where the tectonic loading is stationary. Conversely, in the absence of active faults, it is also risky to consider the lack of micro-seismicity in some areas of the intraplate region as a seismic gap that would indicate the places prone to the next large event. The estimate of seismic hazard for the intraplate domain remains challenging.

Northeastern France in particular is a region subjected to all these debates. The seismic hazard is mainly focussed within the URG due to the Basel earthquake. However moderate events have also been observed in the Vosges, Jura and Ardennes (Figure 1). Each of these sub-regions have a "seismic history" confirmed by the historical catalogues and paleoseismic studies, suggesting that they may remain over time the locus of coseismic deformation. Even if the region of Northeastern France is of relatively small dimensions (<500 × 500 km^2) with respect to other intraplate seismically active regions (Mongolia, New Madrid, etc.), this synthesis shows that many sub-regions have been affected by a distinct tectonic evolution and the seismicity characteristics remain specific to each sub-region, in terms of space and time distribution, magnitude range, and eventually tectonic origin. The analysis of the micro-seismicity for each of them is therefore crucial to mitigate the seismic hazard of this region, characterized by high vulnerability (large cities, industries, infrastructures).

2. Data

We present in the following the main sets of data used for the analysis of the seismicity in the region under study. This latter corresponds to the area located between E001° and E010° longitude and N46° and N51.5° of latitude, excluding the regions of Lower-Rhine Embayment, the Roer graben, the Swabian Jura (East of the Black Forest, see Figure 3 for location) and the northern Alps, which are too far from Northeastern France and from most of the seismic network used for the location of the instrumental seismicity. Datasets acquired in the framework of other specific local studies will be mentioned within the corresponding subsections.

2.1. *Tectonic and neotectonic data*

Investigations in active tectonics have been mainly conducted in the Rhine Graben and the Ardennes [Camelbeeck and Meghraoui, 1998, Meghraoui et al., 2001, Kervyn et al., 2002, Shipton et al., 2016]. The

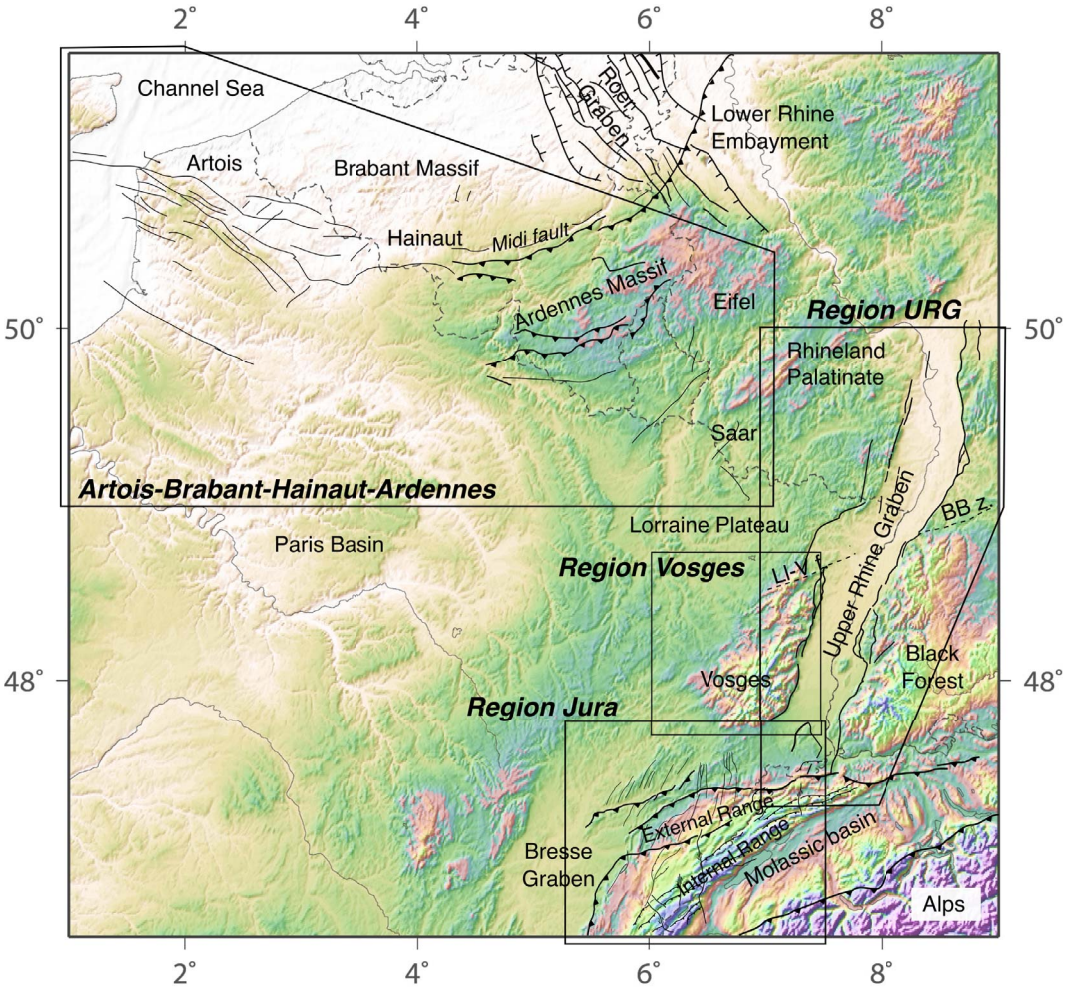

Figure 1. Map of northeastern France and surrounding regions. The rectangles show the sub-regions under study. URG: Upper-Rhine Graben; Ll-V f.: Lalaye–Vittel fault; BB z.: Baden-Baden shear zone.

identification of active faults consists of combined studies in quantitative geomorphology, geophysical prospecting, and paleoseismological analyses (with trenching and isotopic dating). The progress in neotectonic studies has benefited from the recent application of geophysical methods (shallow geophysical prospecting, seismic profiles, etc.). The long-term faulting behavior is determined through systematic studies along each potentially seismogenic rupture-segment to document the earthquake characteristics (fault dimensions, slip/event, slip rate, stress drop, elapsed time and return period of seismic events, seismic moment and moment magnitude) during the Holocene and late Pleistocene. The identification of past surface ruptures in the region is an issue due to the low slip rates (<0.5 mm/yr), the dense vegetation cover on mountains and hills, and the high impact of human activity (urban areas and agricultural ploughing) on the geomorphology in valleys. In addition, the rare indications of recent slip on fault planes are more easily interpreted in terms of normal slip and the identification of strike-slip motion is more complex. This is a crucial point for the faults in our region of interest, since the current stress regime remains debated.

Among the results, the current EU project GeORG consists of a comprehensive geological database dedicated to the Rhine Graben and shows large-scale

3D models that determine the tectonic structures and related georesources. They document late Quaternary tectonic movements along several km long active normal faults [Camelbeeck and Meghraoui, 1998, Meghraoui et al., 2001, Kervyn et al., 2002]. Active faults of the URG are inherited tectonic structure from the beginning of the Neogene some 20 Ma ago [Illies and Greiner, 1979]. Quaternary tectonic activity is documented mostly from previous studies (mainly due to oil exploration) that include numerous seismic reflection surveys and deep wells [Sittler, 1985, Brun and Gutscher, 1992]. Unfortunately, little is known about the structural and tectonic evolution and paleoseismicity of the URG during the late Quaternary, although this is the more critical time period for the study of the active tectonics, and related seismic hazard assessment [Baize et al., 2013, Jomard et al., 2017, Chartier et al., 2017].

2.2. *Seismicity*

2.2.1. *Historical seismicity*

Unlike many regions around the world, the seismic activity in Western Europe has been well documented through several kinds of historical sources, such as private or official testimonies, religious collections, and newspapers. They report large and small shakings that help to evaluate the intensity in the area of the archive. For the French part, we used the catalogue FCAT-17 from Manchuel et al. [2018] which integrated the SISFRANCE catalogue for the historical period [Scotti et al., 2004]. We complement the data of historical seismicity with other regional catalogues. Previous works have documented historical earthquakes of the URG from a thorough examination of archives and documents from cross-border investigations, i.e., between the German, Swiss and French regions [e.g., Perrey, 1844, Sieberg, 1940, Rothé and Schneider, 1968, Vogt, 1979, Lambert et al., 2005]. Macroseismic maps that document the intensity distribution and depth estimates were obtained from the study of historical documents [Levret et al., 1994]. More recently, the historical seismicity of the URG was the focus of detailed investigations from XVIII–XX century press reports (libraries and archives), Fonds Montessus de Ballore, Rothé-BCSF and Vogt archives, German seismological survey at IPG Strasbourg (1892 to 1918), and German regional seismological surveys (Karlsruhe, Stuttgart, Freiburg, etc.).

Regarding the Belgium part, we used the catalogue of the Royal Observatory of Belgium (http://seismologie.oma.be). For the German part, we complement our data set with seismic events from the catalogue compiled by Leydecker [2009].

The period of data is from 782 to 1962. Before 1962, which is the beginning of the instrumental SiHEX catalogue (see Section 2.2.2), we chose to mention the events in terms of MKS intensity.

2.2.2. *Instrumental seismicity*

The French monitoring network in northeastern France developed over decades (Figure 2). From the 60's, the LDG (Laboratoire de Détection et de Géophysique of the Commissariat à l'Energie Atomique—CEA) deployed three stations using one-component short-period sensors, with a telemetric and then a satellite transmission. These stations were complemented over the 70's and 80's by about five short-period and telemetered stations operated by Institut de Physique du Globe de Strasbourg (IPGS). The network, well-adapted to measure the small-magnitude events, remained more or less the same during the following decade, except for the broadband station ECH [operated by Geoscope, Institut de Physique du Globe de Paris (IPGP) and Ecole et Observatoire des Sciences de la Terre de Strasbourg (EOST), 1982], and the specific short-period and telemetered network dedicated to the monitoring of the experimental geothermal project in Soultz-sous-Forêts [Kappelmeyer et al., 1991, Charléty et al., 2007, Dorbath et al., 2009]. In the framework of an Interreg Project, the seismic network grew with the addition of 13 strong-motion sensors, in order to measure the large acceleration of the ground due to the occurrence of large seismic events (Figure 2a). A major densification of the French regional network occurred in the second half of the 2010s with the construction of the Réseau Large Band Permanent (RLBP) of the Grande Infrastructure de Recherche Résif [Réseau Sismologique et Géodésique Français, RESIF, 1995a,b] expected to be complete in 2021 (Figure 2b). The stations have been built in sites of high quality in terms of noise and included broadband sensors in deep holes or in old mines. In addition, eight new stations have been built in the framework of the project EGS (Ecole et

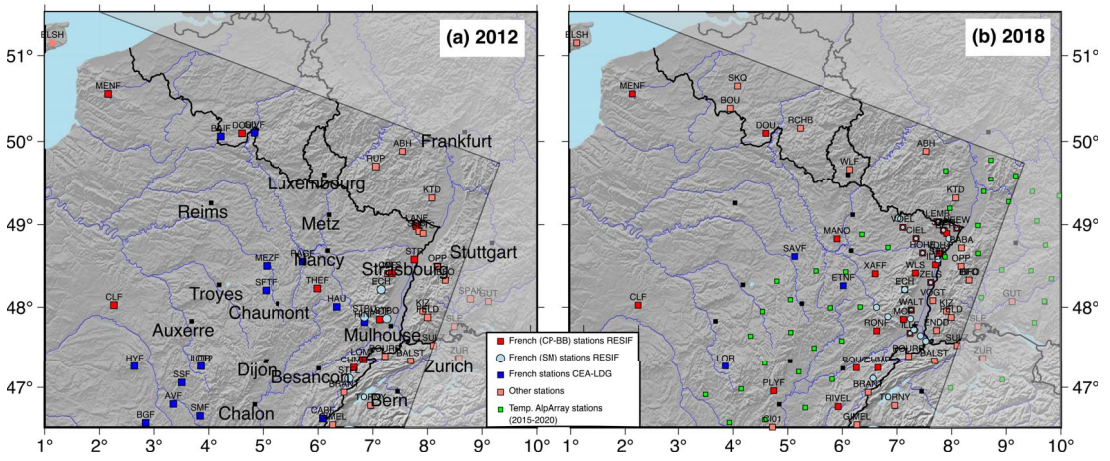

Figure 2. Regional seismic monitoring network used for the hypocentral locations of the Si-Hex catalogue in 2012 (a) and 2018 (b) as examples. For the period before 2009, refer to Cara et al. [2015].

Observatoire des Sciences de la Terre (EOST), Electricité de Strasbourg (ES)), equipped with either middle or broadband sensors in mines or deep holes, with the objective to reduce the detection threshold over the whole Alsace region, where several geothermal plants are developing, and potentially related to induced (micro-)seismicity.

Temporary networks have been installed in the region, but few of the data were integrated to the monitoring system of the Rénass (now called BCSF-Rénass). The data acquired by the recent temporary AlpArray network [AlpArray Seismic Network, 2015] were also used for the location procedure of the Rénass over the period 2015–2020 (Figure 2b).

We use the instrumental seismic catalogue covering the period 1962–2020 [Masson et al., 2021, Figure 3]. This catalogue corresponds to the catalogue initially covering the 1962–2009 period presented by Cara et al. [2005] resulting from the Si-Hex project, which was dedicated to homogenizing the French catalogue in terms of hypocentral location uncertainties and magnitude, expressed as moment magnitude M_w. It has been extended up to 2020. The completeness magnitude improved over time with the densification of the seismic monitoring network in France, but also behind the German, Swiss, Luxembourg and Belgium borders for our area of interest (Figure 3b).

Beyond the borders, the number of stations used for the detection and location process of the Rénass increased over the years, thanks to the collaboration with institutes from Switzerland [CH network, Swiss Seismological Service (SED) at ETH Zurich, 1983], Germany [GR network, Federal Institute for Geosciences and Natural Resources, 1976; LE network, Landesamt Für Geologie, Rohstoffe und Bergbau, 2009], Luxembourg and Belgium [BE network, Royal Observatory Of Belgium, 1985].

The instrumental catalogue counts 8512 events in our area of interest (Figure 3c). The main limitations in building such a catalogue lie in the process of discrimination between natural seismic events and those of anthropogenic origin. Most of the latter correspond to quarry blasts and events induced by industrial activity such as mining or geothermal plant operations. The step of discrimination has not been made during the whole period of the catalogue and remains difficult in post-processing [Renouard et al., 2021].

2.2.3. *Focal Mechanisms and tensors of stress and strain rate*

A total of 216 focal mechanisms (Figure 4) have been used in this study from the new focal mechanism database FMHex20 of RESIF by Mazzotti et al. [2021]. For the region under study, the nodal plane parameters have been either determined by Delouis et al. [1993], Delacou et al. [2004], Vannucci and Gasperini [2004] and Rabin et al. [2018], or estimated by the Seismic Observatory of Northeast France at EOST for earthquakes with low magnitude (2.5 to 4.0). The magnitude of these events ranges

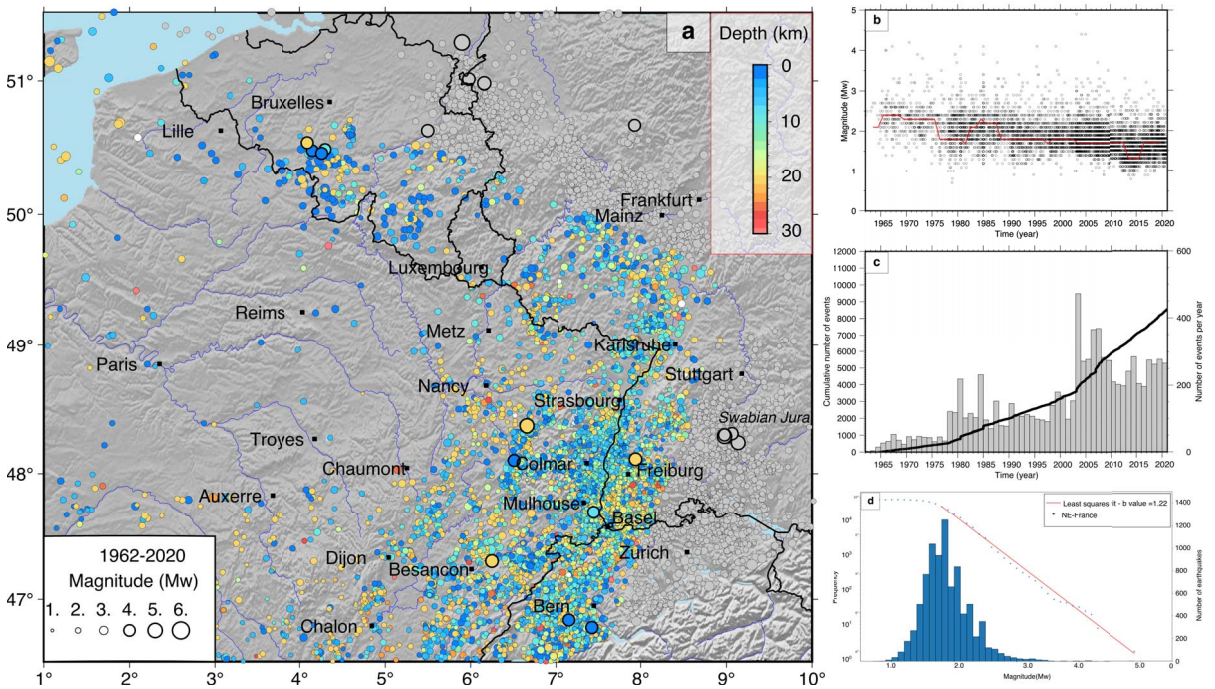

Figure 3. (a) Seismicity from 1962 to 2020 in the northeastern region from the extended Si-Hex catalogue [Masson et al., 2021]. Earthquakes located outside the area of study are plotted in gray. (b) Magnitude of events (dark dots) and completeness magnitude (red line) as a function of time are calculated using the maximum curvature method in a sliding window of two years [Wiemer and Wyss, 2000]. (c) Number of events per year and time evolution of the cumulative number of events located in the region under study. (d) Gutenberg–Richter relation of the cumulative frequency of earthquakes $\log N = a + b\mathrm{M_w}$ for the magnitude range $2.0 < \mathrm{M_w} < 5.0$ in the whole catalogue (the b-value is given in the top right corner) and histogram of magnitude frequency.

from 1.1 to 5.4. We complement the dataset with ten mechanisms from the Hainaut [Camelbeeck et al., 2007] and ten mechanisms from the Brabant Massif [Van Noten et al., 2015] on the French–Belgium border. Most of the mechanisms have been determined using the polarities of first ground motion, and only a few of them using full waveform inversion. We note that data from stations not included for the Si-Hex catalogue might have been used for the focal mechanism determination.

In order to resolve the principal stress directions and the kinematics of faulting for each tectonic domain of northeast France presented below (Figure 5), we conduct the stress inversion from the focal mechanisms compiled in this study. The inversion method consists in the iterative rotational optimization (i.e., the best solution of stress distribution with regards to the fault plane direction and slip vector) as applied in the WinTensor program [Delvaux and Sperner, 2003]. The inversion approach was initially developed from the dihedron method (minimum angle between fault directions and slip vectors that verifies the principal stress direction) as a preliminary solution, subsequently implemented in the rotational optimization used to minimize the misfit between data and model for earthquake fault parameters [Delvaux and Sperner, 2003]. The best fitting stress tensor is derived from fault slip of data set [Gephart and Forsyth, 1984] and is expressed as the direction of the three main stresses σ_1, σ_2 and σ_3, and the R factor $R = (\sigma_2 - \sigma_1)/(\sigma_3 - \sigma_1)$. The direction of shortening (σ_h) is provided, with the number of fault planes compatible with the best stress tensor.

We also estimate the strain rate tensor, following the Kostrov method [Kostrov, 1974], dividing the region into cells of 1° by 1°, using the focal

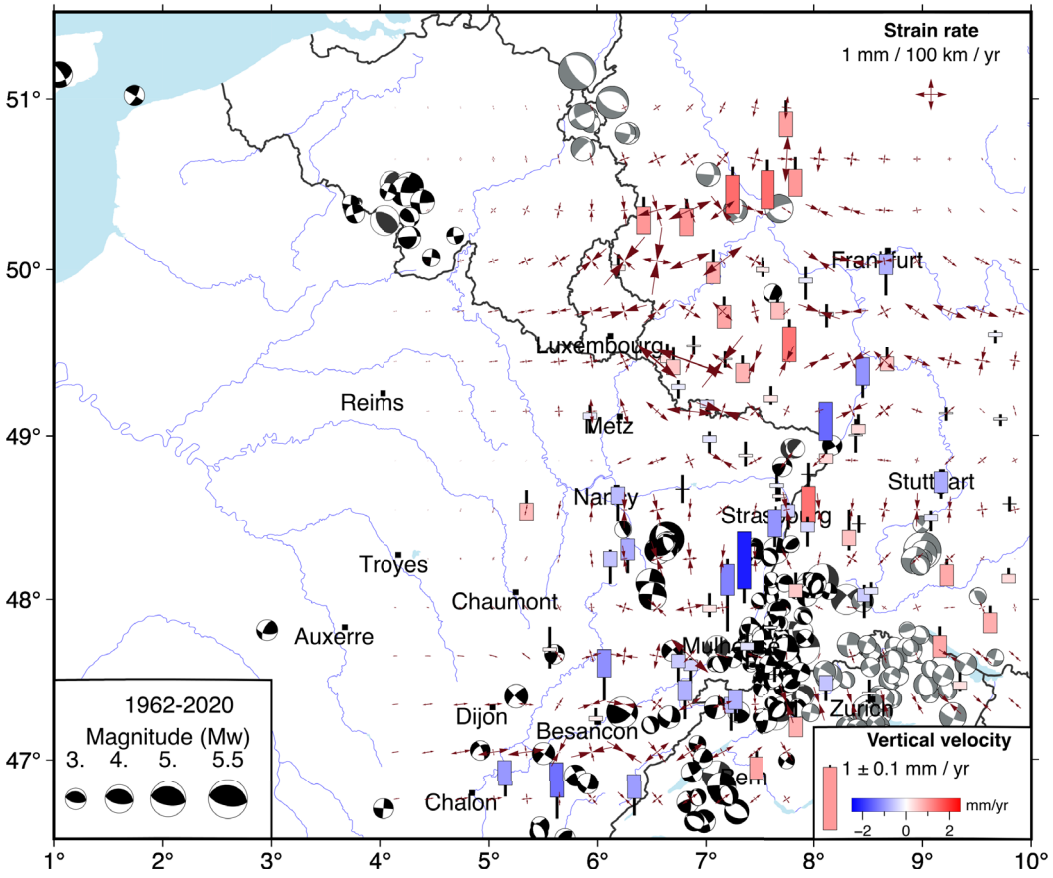

Figure 4. The focal mechanisms considered in this study (in black) from the FMHex20 database [Mazzotti et al., 2020] and other sources (see text). The focal mechanisms located outside our studied area are plotted in gray. The vertical velocities and the strain rate tensors are from Henrion et al. [2020].

mechanisms and the M_w of events in each cell (Figure 5). To do so, we consider a seismogenic depth of ~30 km, homogeneous for the whole region, a shear modulus of 3×10^{10} Pa, and a duration of the catalogue of 60 years. However, because the database is incomplete, we choose to not discuss these results in terms of amplitudes of the strain rates, but only on their style (i.e., compressive vs extensive) and orientation.

2.3. *Surface velocity field and strain rate field*

From the first analysis of the horizontal velocity field at the scale of the European and Mediterranean region, Nocquet [2012] pointed out the lack of relative movements greater than 1 mm/yr across the geological structures in northeast France, such as the Vosges, the URG, and in Belgium. Using both GNSS and leveling data, Fuhrmann et al. [2013] confirmed that the region appears stable, except for a few places where the local surface deformation can result either from tectonic or non-tectonic processes. Since then, several studies conducted at large or regional scale and using longer data time series (more than 20 years for most of them) have confirmed this first order result [Rabin et al., 2018, Masson et al., 2019, Kreemer et al., 2020, Henrion et al., 2020]. Despite a specific processing (filtering, clustering) of GNSS data from the whole of Metropolitan France, Masson et al. [2019] did not detect any clear signal for our study region in both the velocity and strain fields. Henrion et al. [2020] focussed their analysis in the URG and the surrounding regions using the GURN network of GNSS stations in both France [including the RENAG

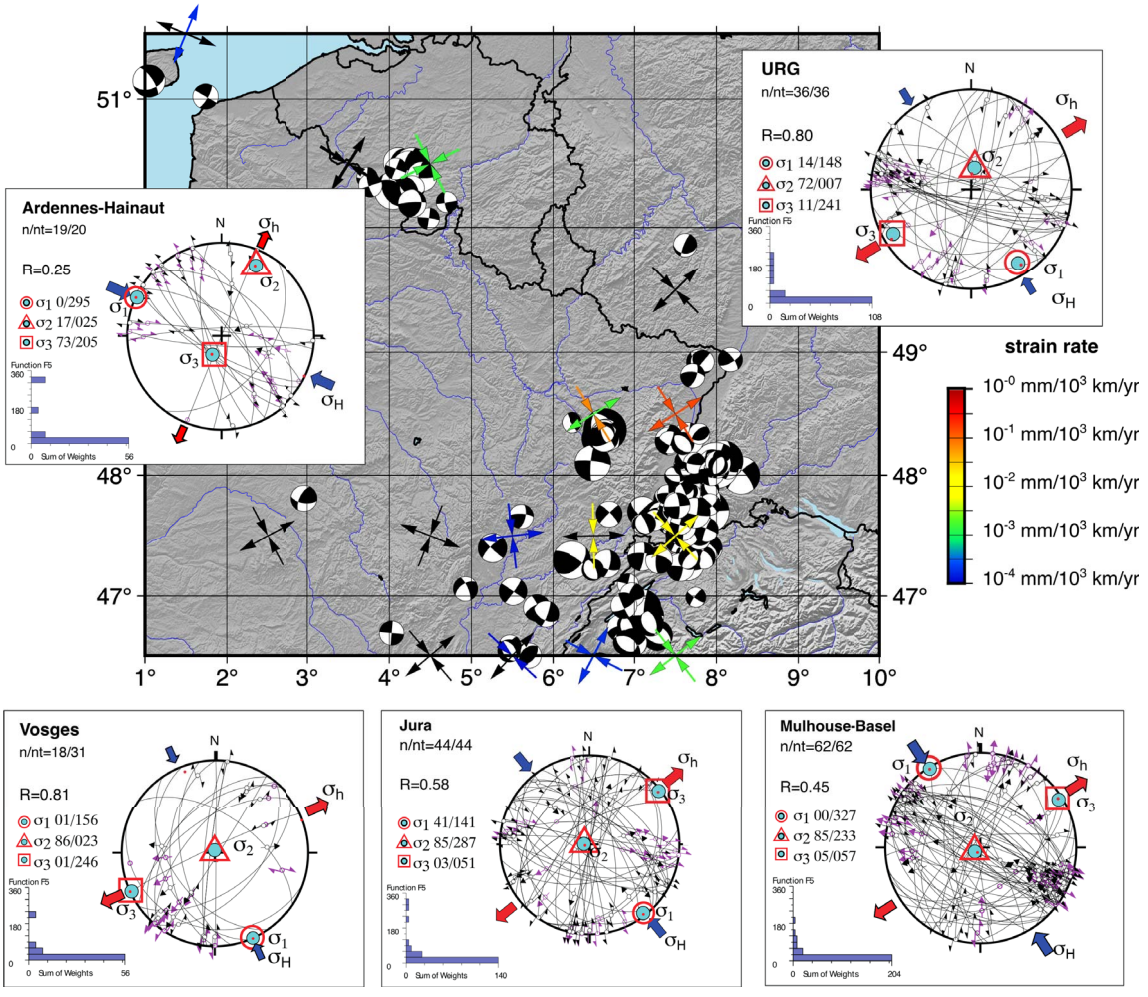

Figure 5. Stress tensor inversion from focal mechanisms for each sub-region. Stress tensors obtained from stress tensor inversion of 182 focal mechanisms of NE France (Jura, Mulhouse/Basel region, Vosges, URG and Ardennes–Hainaut) using the WinTensor program of Delvaux and Sperner [2003]. On a Schmidt projection (lower hemisphere) are represented: the fault planes (black line), the measured and calculated slip vector on each fault (black and purple arrows, respectively), the axes of the principal stresses σ_1, σ_2 and σ_3 (blue dots with red circle, triangle and square, respectively), and the maximum and the minimum horizontal stress (blue arrow and the red arrow, respectively). On the left side are indicated: the number of compatible fault planes used for the inversions (n) over the total fault planes considered for the stress tensor calculation (n_t), the R factor as defined in the text, the dip and strike of the principal stress axes, and a histogram representing the number of iterations (Sum of Weights) with respect to the angle difference between the measured slip and the slip compatible with the best stress tensor on each of the considered fault plane. In each cell of the region, the main horizontal directions of seismic strain rate tensor are deduced from the focal mechanisms. As indicated in the text, the amplitudes have to be taken with caution. For the Ardennes–Hainaut region, we only selected the events that occurred after 1970 in order to exclude the events likely to be mine-induced. Similarly, we did not include the events that occurred during the 2006–2007 period in the geothermal Basel area.

network, RESIF, 2017] and Germany. Rabin et al. [2018] focussed on the Jura using a dataset from permanent stations in the Northern Alps and Jura. Kreemer et al. [2020] focussed on the Eifel volcanic massif, in west-central Germany. In addition, we note the study of Fuhrmann et al. [2015] which presents the first vertical and horizontal velocity fields from a PS-InSAR (Persistent Scatterer Interferometric Synthetic Aperture Radar) analysis combined with leveling and GNSS data for the area of the whole URG and surrounding areas.

In this region, it is important to point out the distinct sources of surface deformation in addition to the possible tectonic loading, and their relative roles on the current seismicity. In particular, the isostatic post-glacial rebound is expected to have an influence on the horizontal and vertical velocity field, as it is observed in northern Europe and northern America [Bogusz et al., 2019], but the related velocities remain below 1 mm/yr over our area of study [Nocquet, 2012, Peltier et al., 2015, Wu and Johnston, 2000].

Henrion et al. [2020] showed the absence of geodetically quantifiable deformation in most of the URG (Figure 4). From the Lorraine plateau west of the Vosges to Württemberg east of the Black Forest, no shortening, extension or vertical relative displacements are sufficiently significant. A few regions exhibit a clear although low deformation. Among them, we note N–S to NW–SE shortening south of the URG, in the area between the Alpine and Jura fronts in Switzerland. This result is confirmed by the study by Masson et al. [2019] and the regional analysis in Jura conducted by Rabin et al. [2018]. Thanks to the decrease of the uncertainties of the vertical GNSS velocities over time, recent geodetic studies show the uplift in the Alps [Nocquet et al., 2016, Masson et al., 2019], and Rabin et al. [2018] underline the progressive increase of uplift from the external range of Jura toward the Alps (Figure 1). The most significant active structure is in Germany, slightly outside our study area, where the vertical motion related to the Eifel volcanic massif (Figure 4), proposed by Henrion et al. [2020] is clearly evidenced by Kreemer et al. [2020]. Once corrected for glacial isostatic adjustment, a ~1 mm/yr uplift associated with local extension surrounded by radial shortening suggest the dynamic role of the mantle uplifting below the volcanic region.

At the scale of the whole region under study, the amplitude of surface velocities remains generally lower than 0.2–0.3 mm/yr. Therefore, even if the uncertainties of the linear velocities deduced from geodetic measurements are decreasing with time, it remains difficult to clearly identify distinct tectonic regions from the velocity or strain rate field.

3. Overall distribution of seismicity in NE France

Northeastern France and its surrounding areas encompass distinct tectonic and geological domains. The earthquakes over the 1962–2020 period (Figure 2) are not distributed homogeneously over the whole region but are concentrated in the four subregions: the Jura, the URG, the Vosges and region at north including Artois, Brabant, Ardennes and Eifel (Figure 1). Although they affect all of these subregions, only a few large earthquakes (i.e., magnitude above 4.0) occurred during the instrumental period. The large majority of the events are crustal (depth <10 km). We note that during the period of the instrumental catalogue the station network is not homogeneous in the considered region, especially in northern France (above the latitude N49°), which explains the small number of low-magnitude events (Figure 2). The Gutenberg–Richter relation shows that the *b*-value of the whole catalogue is 1.22 (Figure 3d). The space–time analysis of the seismicity and its characteristics are discussed below.

We add to this analysis the results of both the inversion of stress tensor carried out for each of the sub-regions and the determination of the axis directions of the main strain rates (Figure 5). One of the main results of the stress tensor inversion is the homogeneity of a strike-slip stress regime for the whole region, except in Ardennes where the stress regime is compressional.

4. Northern Jura

We focus here on the External Range and the High Range of the Jura chain (Figure 1). Located at the northern border of the Alps chain (Figure 6), the Jura chain is considered as the youngest orogen of the Alps, with the northwestward propagation of the thrust front toward the foreland [Becker, 2000, Sue and Schmid, 2017]. The region has been affected by several stages of deformation, including the

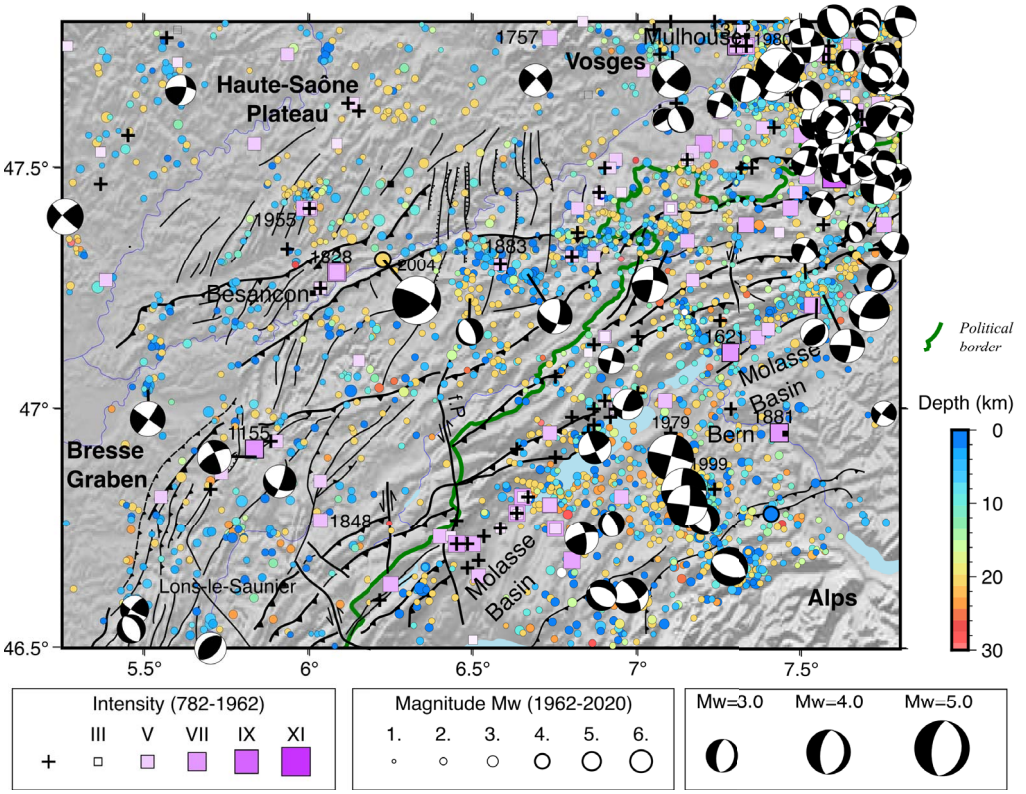

Figure 6. Seismic activity in the region of Jura (see location on Figure 1). The tectonic structures are from Rabin et al. [2018]. f.P: fault of Pontarlier.

Oligocene extension with the formation of the Cenozoic ~N–S-trending Rhine and Bresse grabens followed by the N–S to NE–SW-trending shortening Late Miocene [Becker, 2000, Dèzes et al., 2004]. The Jura belt forms an arc, with a series of thrusts and folds with a bending orientation, from N–S in its southern part (South Jura) where it merges with the subalpine belt, to WSW–ENE in the northern part, in the region of Basel (Figure 6). The Neogene Jura chain is separated from the Alps by the Molasse Basin, and corresponds at north to a cover of Mesozoic and Cenozoic deformed sediments detached from a Palaeozoic basement by a basal décollement of Triassic evaporites. The Quaternary phase of deformation is associated with the northern propagation of the Jura front, with neotectonic evidences of deformation on the northernmost thrusts [Madritsch et al., 2010, Nivière et al., 2006, Nivière and Winter, 2000]. However, the style of deformation remains more ambiguous. The low strain rates over the Plio-Pleistocene and at present [Giamboni et al., 2004, Madritsch et al., 2010], together with the low level of seismicity in the external part of the chain, have not yet helped to better characterize the recent tectonic deformation style controlling the evolution of the orogenic wedge [Rabin et al., 2018]. The debate concerns the transmission of the collision-related compressional stresses into the foreland and the control of the décollement on the basis of this orogenic wedge. Two views are proposed, the thin- versus thick-skinned tectonics, differentiating by the origin of the décollement; the former being consistent with an intra-crustal gently dipping detachment (above the ductile–fragile transition) folding the shallow nappes, the latter invoking a shortening into both the crystalline basement and the cover due to a low-friction deep crustal detachment that could be pre-existing structures in the basement [Piffner, 1990].

In addition to a better assessment of seismic hazard in this region regularly affected by earth-

quakes, the various studies address questions regarding the recent evolution and the tectonics processes involved in the Jura chain front, as a typical example of young orogen forelands [e.g., Lacombe and Mouthereau, 2002, Rabin et al., 2018]. The numerous existing reviews on the seismotectonics of the region are mainly focussed on the Swiss part of the Jura, which is more seismically active than the French, northern one [Houlié et al., 2018, Kastrup et al., 2004]. We note the recent study of Rabin et al. [2018], who combine seismic, tectonic and geodetic data to draw the distribution of the present-day deformation for the High and External ranges of Jura (Figure 1). With the improvement of the geodetic survey and the longer time series of GNSS measurements, it becomes more feasible to estimate the strain field and point out the main zones of active deformation, in order to eventually deduce the structures accommodating it. Specific attention is placed on the existence of seismogenic structures within the underlying basement to better understand the active tectonics of the Jura frontal zones, and assess the relative importance of the orogen-related convergence, the deformation transfer between the Rhine and Bresse grabens and the role of normal and strike-slip faulting in the southern URG (see Section 5).

The region has been regularly affected by a seismicity in both historical and instrumental times. Over the instrumental time, we determine a *b*-value of 1.24 (Supplementary Figure 7a), larger than the one (0.93) from the previous study of Rabin et al. [2018]. The difference of 0.3 between both values can be due to the use of ML and M_w as underlined by Hinzen et al. [2021] for the North Rhine Region. The seismicity is spatially distributed over the whole region with small areas of more concentrated seismic events, without a clear identification of the active faults (Figure 6). A striking feature of the earthquake distribution is the consistency between the historical and the instrumental data sets, since the same active zones are affected by moderate and small events over both time periods (Figure 6). Whereas the area south of the Molasse Basin concentrates a higher number of events with many moderate events in the last decades [e.g., Thouvenot et al., 1998, Kastrup et al., 2004], most of the seismic activity in the northern part is mainly located within the External Range. A denser concentration of events occurs in the region of Mulhouse, where the tectonic structures of the URG interact with the Jura front [Giamboni et al., 2004, Ustaszewski and Schmid, 2007]. In other parts of the region, the epicenters tend to concentrate at the vicinity of the Jura fronts, without clearly underlying the geometry of the thrusts or the major strike-slip faults known to be active in recent times, such as the Pontarlier fault (Figure 6). In the region, among 54 earthquakes with magnitudes ranging between 1.1 and 5.3 of 47 fault planes indicate a stable stress tensor with a N141° E-trending σ_1 and a N051° E-striking σ_3 and an R factor of 0.58 ± 0.1 (Figure 5), consistent with the results of Rabin et al. [2018], though most focal solutions show strike-slip faulting, with very few thrust mechanisms.

Even if the event depth is poorly constrained, the seismicity located south of the Molasse Basin is characterized by the occurrence of deep events (>20 km in depth), that are rare in the High Range and almost absent in the External Range of Jura. This deepening of the seismicity toward the Internal Range is consistent with the observations of Lacombe and Mouthereau [2002], who suggested that the seismicity occurring throughout the entire crust is an indication of the involvement of the basement in the shortening. High fluid pressures are invoked to explain the occurrence of events below the ductile–fragile transition [Deichmann, 1992]. The spatial distribution of stations, particularly in the southwest of the area under study, prevents the reliable determination of numerous focal mechanisms from the distribution of the first polarities, which partly explains their lower number in the region of Lons Le Saunier in addition to a lower earthquake density (Figure 6). The compilation of the focal mechanisms [Mazzotti et al., 2021] for the High and the External Ranges (Figure 1) confirms the dominance of strike-slip events along the Jura chain, which has already been reported by Kastrup et al. [2004] who underline the majority of WNW-trending faults in the High Range and in the southern part. Except for the region in the south of the URG, the low number of events do not allow the estimate of the stress field within the external and high ranges separately. Some attempts have been made by Rabin et al. [2018] revealing a quite homogeneous stress field for the whole region of Jura, with a NW–SE-trending maximum horizontal compressive stress, and a strike-slip regime.

The western part of the Jura chain has been affected by the oldest event which is unclearly reported

in the region of Lons Le Saunier (South Jura) in 1155 with an intensity VII. Two other notable events are dated in 1848 northeast of Lons Le Saunier (V–VI). This part of the front is associated with a network of faults, the Faisceaux Jura, exhibiting Oligocene minor normal faulting related to the Bresse graben formation and reactivated later in the upper Miocene to early lower Pliocene [Chauve et al., 1988, Figure 6]. The distinct rupture types, including one reverse mechanism rarely observed over the whole region suggest the complexity of the tectonics in this area where the transfer zone from the Bresse to Rhine graben and the Jura interact.

The earthquake distribution shows a concentration of events along the frontal zones of the Jura chain and the associated nearby tectonic structures (Figure 6). In the region of Besançon, the two successive NE–SW-trending thrusts concentrate as many seismic events such as within the diffuse network of N–S- to NNE–SSW-trending faults identified nearby. North of Besançon we identify a group of small-magnitude events concentrated in this network of faults over the whole instrumental period at the epicentral location of the three shocks reported in 1955, ~35 km north of Besançon (intensities: VI, VI and IV–V). Further investigations on the mechanisms of these events should be done to verify whether this activity can be seen as the reactivation of Paleaogene normal faults associated with the Rhine–Bresse Transform Zone into transpressional active motion, as suggested by Madritsch et al. [2009] and by the geodetic analysis of Rabin et al. [2018]. Conversely, the epicentral zone of two main events of intensity VI and VII felt by the population near the city of Besançon (Doubs, city of Thise) at the end of October 1828 suggests the activity of the thrusts. This is also the case for the largest earthquake of the region, known as the Roulans event of 23 February 2004 with a M_w estimated to 4.4 (maximum intensity VI, also called the Baumes-Les-Dames or Rigney event). Located at the frontal zone of Jura, this event was characterized by the absence of aftershocks and a focal mechanism consistent with a strike-slip motion (left-lateral component on the SW–NE-trending fault plane) with a slight reverse component. The region east of the Roulans event (E006.6–E007°) is characterized by numerous earthquakes occurring at shallow and intermediate depth and at the location of the historical event reported in 1883 (intensity V). This seismicity is low but regular over time with some picks of activity lasting for one or for a couple of days, such as the sequence of 19 earthquakes on 11 March 2019 with a magnitude ranging from 1.7 to 2.3.

The geodetic measurements have been motivated to detect the ongoing active collision on the Jura [Jouanne et al., 1995, Walpersdorf et al., 2006, Delacou et al., 2008, Nocquet et al., 2016, Rabin et al., 2018, Houlié et al., 2018]. Due to the low strain rate of the region, the quantification of the surface movements remains complex since they are of the same order as the uncertainties over the short term, but also over the long term. Evidence of Quaternary deformation has been identified by neotectonic studies across the northernmost thrusts of the Jura in the External Range [e.g., Nivière and Winter, 2000, Giamboni et al., 2004, Nivière et al., 2006, Ustaszewski and Schmid, 2006, 2007, Madritsch et al., 2010], which seems to be underlined by the current seismicity (Figure 6).

5. Upper-Rhine Graben

The Upper-Rhine Graben is a ~N–S trending sedimentary basin that was initiated during the Oligocene. Subsidence and synrift sedimentation started in Eocene. The reflection profiles ECORS DEKORP [Brun and Gutscher, 1992] gave an image of the crust and the upper mantle in the region. Two lines have been acquired across the URG and have revealed the doming of the Moho below the URG, the asymmetry of its structure, consistent with a normal shear zone cross-cutting the lower crust and the Moho at depth, and the variations of thickness of the Tertiary synrift sedimentary deposits within the basin. The asymmetric rifting is controlled by larger fault displacements, leading in particular to deeper Neogene and Quaternary formations in the eastern flank [Brun and Gutscher, 1992, Illies, 1981]. Fault zones form north–south trending steep and composite scarps bounding the eastern and western flank of the northern URG (Figure 7). Faults appear as a geomorphic lineament structure that separates a higher plateau of basement Hercynian rocks (Black Forest and Vosges Mountains) from lower levels of alluvial fans and fluvial Rhine units in the graben. Early mapping of faults in the basin has been done from seismic reflection and hydrocarbon exploration profiles [e.g., Illies, 1981, Behrmann et al., 2003].

A few studies have focussed explicitly on Neogene and Quaternary fault movement [Haimberger et al., 2005, Meghraoui et al., 2001, Lemeille et al., 1999]. Later, the likelihood of late Pleistocene and Holocene earthquake activity in the region has increasingly being investigated [Kervyn et al., 2002, Ferry et al., 2005, Peters et al., 2005, Nivière et al., 2008, Baize et al., 2013].

Due to the high density of stations of the French monitoring in Alsace plain and surroundings, particularly in recent years (see Section 2.2.2), the instrumental seismicity accounts for more than 5000 events over the whole region, with a magnitude ranging from 1.1 to 4.1, and a completeness magnitude from ~2.5 at the beginning of the catalogue (60's) down to 1.3 in recent years. We calculated a *b-value* of 1.38 for the whole URG (Supplementary Figure 7b), which is higher than the range calculated from ML magnitudes for the central, southern of northern URG (0.92, 1.42 and 1.06, respectively) by Barth et al. [2015], who also take the historic seismicity, i.e. large events, in their analysis. We note that the large intensity of the felt events in the historical catalogues may be due to the effects of the unconsolidated sedimentary cover within the Alsace plain, as instrumental measurements at depth and surface showed in the S-URG [resonance and surface amplification; Trampert et al., 1993].

The instrumental and historical seismicity in the URG region, and the spatial distribution of the earthquakes reveal two striking features (Figure 7). First, the large majority of the epicenters from both catalogues are primarily concentrated within the graben, where most of the hypocenters are in the first 10 km below the surface. In comparison, and for the time-window under analysis, the margins of the graben appear more quiet, except for the southeastern margin of the URG, the southeastern Black Forest (BF), where a constant seismicity is recorded, with events of higher magnitude and/or intensity (i.e., larger than M_w 4). Second, we observe a difference of earthquake concentration between the southern URG (S-URG) with a higher density of recent micro-seismicity and the northern URG (N-URG) with areas almost devoid of events over the last 60 years (Figure 7). Figure 8 illustrates this difference in terms of both density of events and cumulative seismic moment. The lack of large earthquakes in the N-URG with respect to the S-URG is underlined by the distinct b values of 1.33 and 1.52 for the S-URG and the N-URG, respectively (Supplementary Figure 7c, d).

5.1. *Southern Upper-Rhine Graben (S-URG)*

The regional seismic activity necessarily includes the largest event of the region which occurred in Basel in 18 October 1356, with I_{max} of IX–X (Figure 7b). This event has been preceded by other shocks of large intensity (>VIII MKS), such as in 1021 (12 May; I_{max} = IX; Basel–Mulhouse), 1346 (24 November, I_{max} = IX; Basel), and a subsequent event in 1531 (26 January; I_{max} = VIII; Basel–Mulhouse), which have been documented by Perrey [1844], Sieberg [1940] and Rothé and Schneider [1968]. With effects felt up to a distance of 120 km distance, the serious damage due to the 1356 event was reported in many castles and churches up to 50 km in the epicentral area [Meghraoui et al., 2001, Fäh et al., 2009], although revised analyses tend to refocus the damaged area in the vicinity of the town of Basel [Lambert et al., 2005]. Various methodologies (archeology, history, paleoseismology and modeling of seismic intensities, refer to Fäh et al., 2009) have been applied to study this large and damaging event, mainly to determine its location and the dimensions of the seismogenic fault, and eventually estimate the seismic hazard within the intraplate domain of western Europe. In case of the 1356 earthquake, several sources can be invoked: normal or strike-slip slip on a normal fault associated with the URG, slip along the detachment of the northern Jura Front or the reactivation of an ancient fault in the basement [Ustaszewski and Schmid, 2007]. Whereas Meyer et al. [1994] proposed the reactivation of a basement fault using analyses of topographic data, satellite and aerial images, Meghraoui et al. [2001] identified the surface expression of an active NNE-trending normal fault (Basel-Reinach fault) south of the town from geomorphic features, drainage pattern and paleoseismic trenching. In addition, Ferry et al. [2005] evidenced ruptures affecting late Pleistocene and Holocene deposits from paleoseismic investigations in trenches and dating, suggesting episodic intraplate earthquake activity with a relatively long return period (>2500 years). Several magnitude values have been proposed, from M_w 6.5 to 7.1 [Mayer-Rosa and Cadiot, 1979, Meghraoui et al., 2001, Fäh et al., 2009]. Several events of maximum intensity of VI to VII supposed to be located in

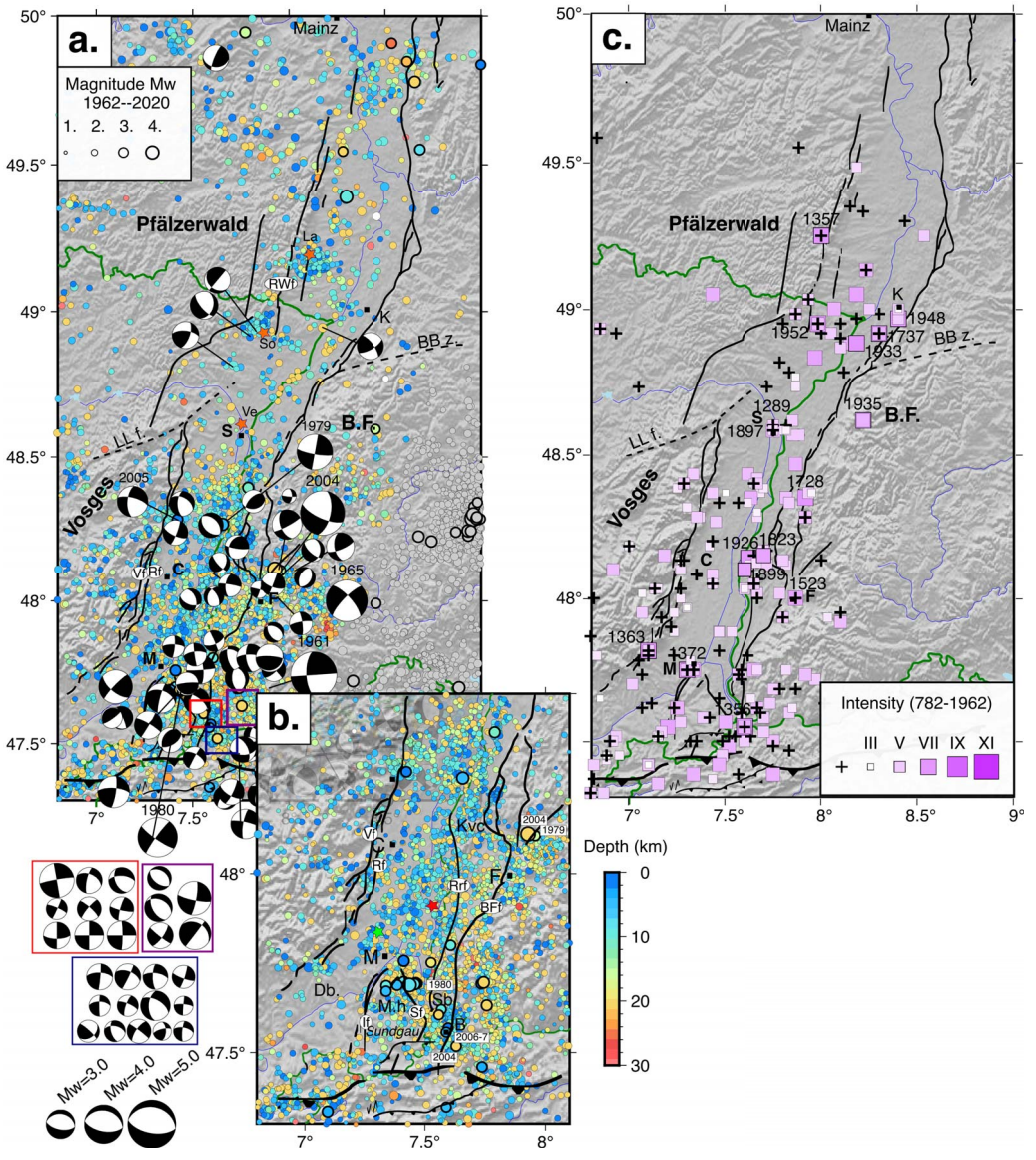

Figure 7. Seismic activity in the region of the URG (see location on Figure 1). Ll-V. ff.: Lalaye–Vittel fault. BB z.: Baden-Baden shear zone. B.F.: Black Forest Massif. (a) Instrumental seismicity [1962–2020] with focal mechanisms. (b) Zoom on the southern part of the S-URG. (c) Historical seismicity. Towns: B.: Basel; C.: Colmar, F.: Freiburg; K. Karlsruhe; M.: Mulhouse; S.: Strasbourg. Regions: BF: Black Forest; Db: Dannemarie basin; Mh: Mulhouse horst; Sb: Sierentz basin. Faults: Sf: Sierentz fault; If: Illfurth fault; Vf: Vosges fault; Rf: Rhine fault; Rrf: Rhine river fault; BFf: Black Forest fault; Rwf: Riedseltz–Worms fault. Green star: location of the surface displacement measured in Staffelfelden, near the Mines de Potasse d'Alsace; Red star: Fessenheim nuclear power plant; Orange star: Ve: Vendenheim geothermal stimulation site (note that the events related to the 2019–2021 sequence are not plotted, refer to Schmittbuhl et al., 2021); Orange star: So: Soultz-sous-Forêts/Rittershoffen geothermal sites; Orange star: La: Landau geothermal site.

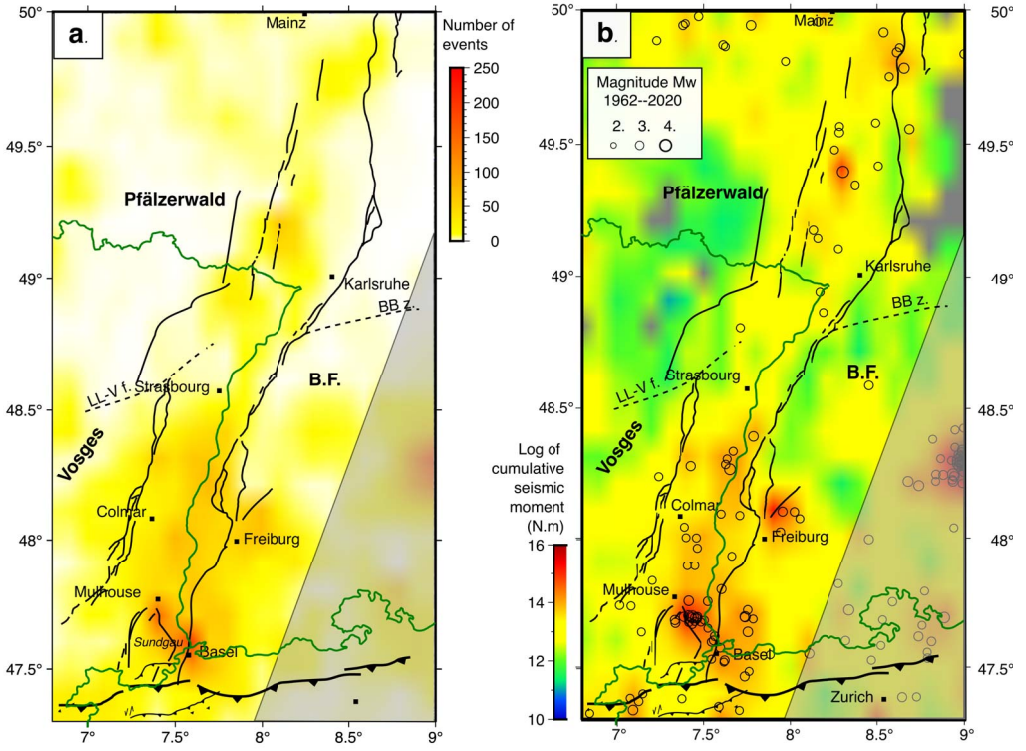

Figure 8. (a) Earthquake density over the URG region and (b) cumulative seismic moment. Both values are calculated in a 0.1° × 0.1° sliding window. Only earthquakes with M_w above 2.7 are plotted in b. Black lines are Quaternary faults.

the same area are reported in the historical catalogue (1428, 1559, 1610, 1650).

The Figures 7(b) and 8(a) show that the region of Basel concentrates the largest number of recent instrumental events. This is mainly due to the seismic sequence that started in December 2006 and which was induced by the fluid injection 5 km below the town of Basel [Deichmann et al., 2014]. In local catalogues, more than 13,000 events have been detected with the local network during the phase of stimulation for the geothermal reservoir enhancement but also over the next six years [Kraft and Deichmann, 2014]. Except for the main shock which reached a M_w of 3.0 and a couple of aftershocks within this specific sequence, only one event located here has a magnitude M_w above 3.0 (21 June 2004; $M_w = 3.1$).

However, two neighboring regions have been affected by $M_w > 3.0$ earthquakes: the region of Mulhouse with the occurrence of the sequence of Sierentz [Rouland et al., 1983] and the southwestern corner of the Black Forest, northeast of Basel. The Sierentz sequence has been studied through a local temporary network deployed a couple of hours after the main shock occurred ($M_w = 4.8$, I_{max} = VII, Figure 7b) on 15 July 1980 at a depth of ~13.5 km [Rouland et al., 1983]. Except for an event of magnitude $M_w = 2.5$ which occurred six months earlier, the area was not particularly seismically active before the sequence in comparison to the region bordering the Black Forest. The large measured intensity has been interpreted as the effect of the thickness of the sedimentary layer in this region of the basin [Rouland et al., 1983].

A catalogue of focal mechanisms has been built from this experiment, and later completed by a new set presented in Maury et al. [2013]. The main event showed a strike-slip mechanism with subvertical planes, as most of the aftershocks do [Figure 7a; Rouland et al., 1983, Bonjer, 1997]. Many tectonic structures have been identified in the region called Sundgau (Figure 7b), South of Mulhouse, where the horst of Mulhouse "splits" the southern end of the URG into two Quaternary grabens of Dannemarie

(Db) and Sierentz (Sb, also called Allschwil Basin), to the west and east, respectively [Nivière and Winter, 2000]. Figure 8 shows that this latter graben concentrates the higher density of earthquakes and the locus of the largest cumulative seismic moment of the whole URG region. The shallow and intermediate seismicity located in the area during the 1980 sequence of Sierentz or over the whole period of the Si-Hex catalogue could reflect the activity, or reactivation, of these faults, in particular the NNW–SSE-trending Sierentz fault (Sf) bounding at East the Mulhouse horst (Figure 7b). We note in contrast the current quiescence of the area corresponding to the hanging wall block of the Illfurth fault (If) bounding at East the Mulhouse horst [Mh, Ford et al., 2007]. However, a deeper analysis of the seismicity is required to attribute this seismicity to specific active faults, since contrasts of seismic velocities from local tomography together with analysis of seismic profiles and gravimetry evidenced as well NNE–SSW-trending faults in the upper basement and the sedimentary cover [Lopes Cardozo et al., 2005]. Using 62 focal mechanisms of earthquakes with magnitude ranging between 1.7 and 4.8, the stress analysis indicates a strike-slip regime, with σ_1 trending N147° E and σ_3 striking N057° E with an R factor of 0.45 ± 0.1, consistent with other stress inversions obtained for the region [Figure 5, Plenefisch and Bonjer, 1997, Kastrup et al., 2004].

The current stress regime and its variations on space and at depth in this area are still debated [Delouis et al., 1993, Plenefisch and Bonjer, 1997, Maury et al., 2013, Kastrup et al., 2004, Rabin et al., 2018, see Discussion]. In the region of Mulhouse, several historical events have been recorded, including the event of I_{max} = VII in 1372, and micro-seismicity is regularly located (Figure 7b, c). An anthropogenic origin of the instrumental earthquakes might be supposed, due to the underground activity of the Mines de Potasse d'Alsace (depth ~500 m). Recent measurements of SAR interferometry detected localized zones of subsidence over the mining concessions, with high amplitude (>8 cm/yr) during the period of exploitation up to 2002, and over the post-mining period as well with decreasing velocity rates, currently lower than 5 mm/yr [Modeste et al., 2021]. Specific localized signals could be associated with the reactivation of small faults within the Potassic Basin, such as in Staffelfelden (Figure 7b).

In the south of the Black Forest, hypocenters occur deeper (~20 km) than in the S-URG, suggesting seismogenic structures within the basement, even in the lower crust, as proposed by Bonjer [1997] using structural data from seismic reflection profiles. The historical seismicity also shows a concentration of known shocks in this region with intensity remaining below VI. Further north, the central part of the Black Forest (latitude ~N48°) is regularly affected by earthquakes. Over the historical period only one event exceeded the I_{max} = VI in 1523, whereas the Waldkirch earthquake (5 December 2004; M_w = 4.4) is the largest recent event of the whole URG region. At the same location as the 1979 event (7 January, M_w = 3.1), this moderate event has been also followed by a sequence of aftershocks reported by Häge and Joswig [2009], who showed from the hypocenter's alignment at a depth of ~11 km, a WNW-ESE direction, consistent with the direction of the nodal plane of the focal mechanisms (Figure 7a) and of the Late-Cretaceous faults and dykes present in the Massif of the Black Forest.

West of the Black Forest, the earthquake distribution within the S-URG is characterized by a difference of concentration along the western and eastern margins of the S-URG. The events included in the instrumental catalogue concentrate along its eastern border faults (Figure 7a). Conversely, at this latitude of the graben (N47.6 to N48°), the historical catalogue reports more events along the western border of the S-URG, at the border with the Vosges, with events of low intensity except for the event of intensity VII in 1363 (Figure 7c). The western margin is structured by a system of two large faults (Figure 7a), the Rhine and Vosges faults (Rf, Vf) associated with the formation of the S-URG, and affected by various stress regimes since then, with a still debated transpressional period during the uplift of the Vosges Massif [e.g., Rotstein et al., 2005, Lopes Cardozo and Behrmann, 2006, Rotstein and Schaming, 2008]. Their current activity remains unclear, even if a recent activity can be observed along a few seismic reflection profiles [Rotstein and Schaming, 2008], including in the southwestern region, where the western border of the S-URG reorients along the NE–SW direction.

The recent geodetic strain rate field and vertical velocity field do not allow us to localize a zone of active deformation, for either the western or eastern

border of the S-URG [Henrion et al., 2020; Figure 4], and no active subsidence is clearly evidenced today, unlike over the Quaternary with the large thickness of sediments in the URG [Illies, 1981]. Quaternary tectonic activity appears clearer for the eastern border of the S-URG, although several faults are potentially responsible for the intense seismic activity, characterized by the lack of large events in the instrumental time (M_w < 2.8 in the region in the URG from Mulhouse up north for ~50 km). The largest structure corresponds to the BF fault forming a topographic slope along which the basement of the BF Massif is outcropping. However, geomorphological and geophysical investigations suggest that the current tectonic activity is concentrated further west, along the Rhine River fault within the plain of the S-URG [Figure 7b, Nivière et al., 2008, Thomas et al., 2017]. Both of these faults are associated with (vertical) offsets in the leveling lines measured from 1922, although a part of the deformation could correspond to local effect due to the mining subsidence [Fuhrmann et al., 2013]. The Rhine River fault draws particular attention due to the proximity of the recently shut down Fessenheim nuclear power plant, and the estimate of its seismogenic behavior is of great importance with regard to the seismic hazard of the region [Jomard et al., 2017, Chartier et al., 2017]. Several historical earthquakes which have been related to the Miocene volcanic Kaiserstuhl complex, west of Freiburg, could be attributed to the Rhine River fault. Among them, Fracassi et al. [2005] reported the sequence of 1926 (June, I_{max} = VII) including pre- and aftershocks, and a collection of events with intensity VI–VII (1523, 1823, 1899).

Between Colmar and Strasbourg, the earthquake density increases from the western to the eastern margin of the graben, in both historical and instrumental catalogues. The largest event of this central part of the URG occurred in 1728 (3 August, I_{max} = VII, Lahr/Mahlberg event) along the eastern border of the graben, among a sequence of eight events with intensity between V and VI. The recent seismicity shows deeper earthquakes in the eastern side of the graben. Various types of focal mechanisms can be observed, from normal faulting along NW-trending planes, reverse faulting along NE-trending fault and left-lateral strike-slip events along ~N–S-trending planes (or right-lateral strike-slip events along ~E–W-trending planes; Figure 7a), such as the largest events of the area at Rhinau in 1979 and in 2005 (M_w = 3.7 and 3.2, respectively; Figure 7a).

5.2. *Northern Upper-Rhine Graben (N-URG)*

The region of Strasbourg is particularly interesting in light of the recent seismic sequence in 2019–2021 in the north of the city of Strasbourg. Though the micro-seismic activity started in 2018, the first felt event occurred on 12 November 2019 (M_w = 3.0). The subsequent sequence encompasses more than 1200 events, including the earthquakes of magnitude M_w 3.6 and 3.3 felt on 4 December 2020 and 22 January 2021, respectively. Several historical events were reported for the area of Strasbourg, in 1289 (I_{max} = VI) and in 1897 (I_{max} = VI). Given that the recent sequence has doubtless been induced by the geothermal industrial activity (epicenters in close vicinity to the wells, hypocentral depth similar to the depth of the wells), the potential natural and human-induced reactivation of faults with long loading periods is of primary importance in this densely urban area. A detailed analysis of this sequence presents the space–time evolution of the hypocentral distribution [Schmittbuhl et al., 2021]. Two main clusters characterized this sequence: the relatively large distance between the first one and the well location, and a delay between the injection tests and the onset of the sequence. Both suggest a hydraulic diffusion along the fault. The two main clusters are aligned along a N–S-trending fault, consistent with the direction of the focal planes of the mechanisms of the sequence [Schmittbuhl et al., 2021]. The fault activated during this sequence was known from seismic profiles (http://www.geopotenziale.org), and belongs to the network of faults vertically offsetting the reflectors in the Quaternary sediments at the center of the N-URG, leading to an estimate of low slip rates [<1 mm/yr; e.g., Bertrand et al., 2006]. We note as well that two 1935 earthquakes (I_{max} = VI and VII) located on the eastern margin of the URG, in the Black Forest, have been relocated by Fracassi et al. [2005] to the region of Offenburg, at the center of the N-URG, where other indicators of Quaternary fault activity have been identified (Figure 7b).

Further north, seismic clusters at the center of the URG can also be attributed to the geothermal industries, around Soultz-sous-Forêts in France and Landau in Germany (Figure 7b). However, we note

that most of the events have been discriminated, and most of the earthquakes located in this area of the N-URG, are attributed to either the eastern or western border faults.

In 1933 the Rastatt/Seltz event (I_{max} = VII) occurred south of Karlsruhe, along the eastern border fault of the N-URG, where several historical events have been located and follow this latter fault (the sequence of 13 events in 1737 I_{max} = V to VII; 1871 I_{max} = V; 1763 I_{max} = VI; 1903 I_{max} = VI–VII; two events in 1948 I_{max} = V and VII; Figure 7b).

On the western border of the N-URG, near the area affected by the 1763 event (I_{max} = VI), the earthquake sequence of 1952 shows a southern migration of the macroseismic area, with an initiation on 2 February (I_{ma} = VII, MKS, ML = 5.2) in the northern area near Mannheim in Germany, a second shock on 29 September (I_{max} = VII) with maximum damage between Landau and Wissembourg in France, and a third shock on 08 October (I_{maw} = VIII) with maximum damage between Wissembourg and Haguenau in France (Figure 7b). The detailed damage investigations, isoseismal shape and inferred epicentral location lead to a shallow hypocentral depth (<8 km). Located along the graben's western shoulder, this seismic sequence also follows the ~110-km-long Riedseltz–Worms fault zone belonging to the late Pleistocene structures visible in seismic profiles and tectonic features mapped by Illies [1981]. Exposed outcrops of faulted late Quaternary units (loess, <30 ka), prominent and linear scarps on alluvial fans and geomorphic markers of drainage control along the fault zone imply the occurrence of late Pleistocene and Holocene faulting. The most recent tectonic geomorphology is documented through faulted and tilted (high angle) late Quaternary units with triangular facets bounding the Vosges Mountain front [Shipton et al., 2016]. Immediately south of the French–German border the fault is exposed in quarries and affects Pleistocene sands overlain by 0 to 10 m of undifferentiated loess of late Wurm age [<30 ka, Doebl, 1970, Bano et al., 2002]. The fault extends further north and follows the mountain front within the basement rocks of the Vosges Mountains to form a prominent escarpment in the Quaternary units of the northern URG until Mainz region [Peters et al., 2005, Peters and van Balen, 2007, Shipton et al., 2016]. Although made of moderate earthquakes, the 1952 seismic sequence shows the potential for M_w 6.5–7 earthquake in the northern URG [Shipton et al., 2016]. To the northeast of the URG, the thickness of the Quaternary terrestrial clastic sediment sequences is variable with a maximum of 200 m [Doebl, 1970]. This limited thickness of Quaternary formation along the URG testifies to a tectonic history with an estimated low level of uplift rate (~0.1–0.3 mm/yr) in the last Ma.

Within the N-URG, two clusters of shallow (<5 km) earthquakes located near both geothermal plants in Soutz-sous-Forêts and Landau underline the complexity of the seismic activity in this region (Figure 7b). First, even if the discrimination between natural and induced earthquake has been done for the instrumental catalogue, numerous events still remain and further analysis should be done with more criteria to properly flag those recognized as induced events. Second, both regions have a background seismicity with deeper locations (>5 km) located at the vicinity of known late Quaternary faults [Weidenfeller and Zöller, 1995], where geological and geomorphological markers (triangular facets attest to recent slip, likely related to tectonic deformation).

The historical and instrumental earthquake distribution in the northern URG indicates a clear lack of moderate to large seismic events and therefore a seismic gap that may depend on the episodic behavior of active faults in intraplate tectonic domain. Paleoseismic results show that return periods for earthquakes similar to the 1356 Basel event are of the order of 2500 years [Ferry et al., 2005]. Considering that reliable historical seismic records may not date back to more than 1000 years, it implies that other large undocumented earthquakes in the region may be missing in the seismicity catalogue.

6. Vosges

The region of the Vosges encompasses the sandstone mountains in the north and the Hercynian Vosges Massif located between the Parisian sedimentary basin and the Cenozoic Upper-Rhine Graben (Figure 1). To the west, in the Lorraine Plateau, the Triassic layers lie unconformably on the Vosges basement, when large NNE-trending normal faults shaping the URG form the eastern boundary of the Vosges. The Hercynian Vosges Massif is usually divided into two main domains: the northern domain (Saxothuringian zone) consisting of metamorphics

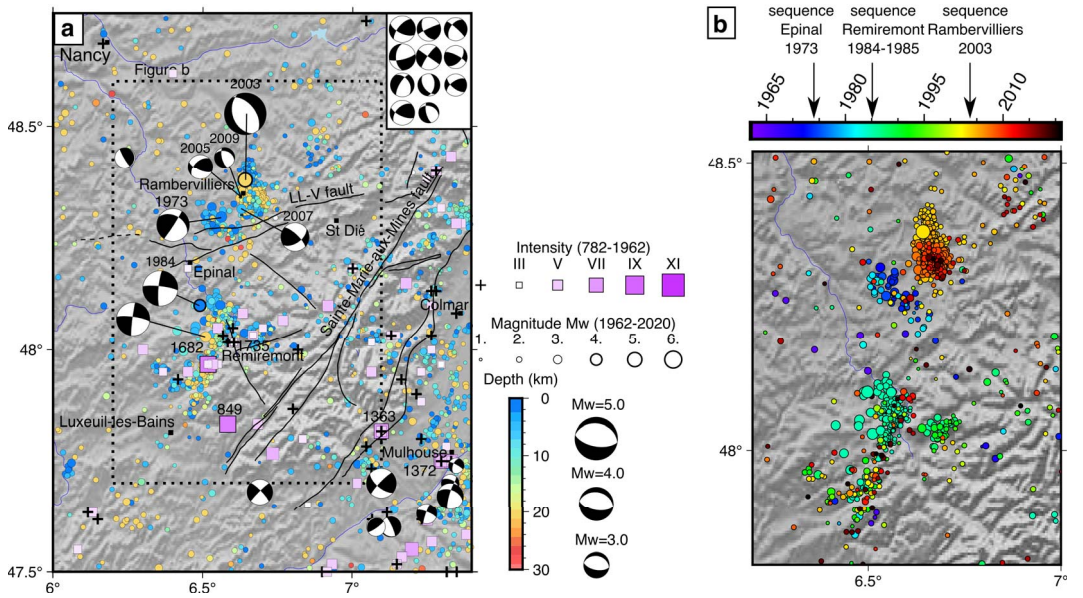

Figure 9. (a) Historical and instrumental seismicity in the Vosges region, together with the focal mechanisms (see location on Figure 1). LL-V fault: Lalaye–Vittel fault. (b) Space–time evolution of the instrumental seismicity in the western Vosges.

and granitoids, and the southern domain (Moldanubian zone) consisting of Palaeozoic sediments and volcanic rocks affected by the Variscan orogen. The limit between those two domains corresponds to the Vittel fault or the Lalaye-Line (LL) right-lateral shear zone, which is also present east of the URG shifted by 30 km to the north, in the northern Black Forest (Figure 6). The crystalline massif of Black Forest forms the eastern shoulder of the URG. In the Hercynian Vosges, the two main tectonic structures are then the LL shear zone and the ~NNE-trending fault of Saint Marie aux Mines crossing the whole crystalline massif as an exhumed and inactive ductile left-lateral shear zone (Figure 9).

The seismic activity is mainly concentrated at the western edge of the crystalline massif (Figure 9). Several sequences have affected this area, with events of intensity and/or magnitude significant with respect to the Metropolitan seismicity (i.e., intensity above VII and M_w above 4.0). Despite the lack of clear evidence of active deformation on the surface, both the historical and the instrumental seismic catalogues show that this area remains over time a seismogenic zone associated with a moderate seismic hazard. All the epicenters are concentrated within a 100 km long and NNE-trending band more or less parallel to the NE-trending LL shear zone (Figure 9b). Two specific main zones are identified: one located near the town of Remiremont in the south, and one near Rambervilliers in the north (Figure 9a). These sequences do not share similar characteristics in the evolution of the seismicity, such as the duration of the sequence and the space–time distribution of the events. Regarding the southern zone, the largest event of the historical catalogue occurred in 1682 near Luxeuil-les-Bains, with an intensity of VIII. This earthquake, felt up to 400 km away, including Paris, has marked the population by the damage and the state of panic that it induced. Although little information is available, a similar event of the same intensity has been reported in the same area in 849, and a smaller one in 1735 (intensity V).

The instrumental time encompasses a significant number of moderate earthquakes, as shown by an intermediate *b-value* of 1.22 for the whole catalogue (Supplementary Figure 7e). A seismic sequence was located near Remiremont in 1984–1985 and lasted at least three months. After the occurrence of several aftershocks at the beginning of December 1984, the major event reached a magnitude of M_w = 4.1

(ML = 4.8) on December 29, 1984. The second part of the sequence has been monitored with the deployment of a temporary dense network [Haessler and Hoang-Trong, 1988]. This allowed the estimate of the focal depths between 6 and 8 km with a small uncertainty (500 m), and the precise mapping of the spatial distribution of the earthquakes along a 3 km long and ~N–S-trending band, in agreement with the vertical plane of the focal mechanisms showing a left-lateral slip (Figure 9a). Further investigations revealed lateral migration of the seismicity along this plane during the sequence [Plantet and Cansi, 1988].

Regarding the northern zone, the "sequence of Epinal" in 1973 corresponds to a series of ~20 shocks occurring over the whole year, with magnitudes ranging from 1.7 to 3.8 (22 February 1973), a few shocks in the two following years (M_w 3.3 in 12 November 1974) and a small sequence of ~15 events in March 1981, with magnitude ranging from 1.9 to 2.8. A similar sequence occurred only 5 km south of the area activated in 2003 in Rambervilliers with the occurrence of the major shock (22 February 2003) with a M_w = 4.9, being the largest earthquake recorded in the region during the whole instrumental time. The effects of this event have been felt up to 300 km, and damage has been reported in the region [Cara et al., 2005]. This large event was located at a depth of ~12 km, and was followed by a sequence of aftershocks migrating toward the surface with focal mechanisms more or less consistent with the main shock, corresponding to normal faulting on a N315° E-trending and 45° N-dipping plane and a subsequent swarm [Got et al., 2011]. Many focal mechanisms have been computed from the immediate sequence of aftershocks using a temporary seismic network deployed after the main shock. Since then, seismic activity has been recorded in the same area till 2011, with a large number of events in the Si-HEX catalogue (up to 240 events for the year 2009).

The seismicity located at the western edge of the Vosges occurs through sequences limited in time and remains spatially concentrated at the location of the outcropping contact of the sedimentary cover and the Hercynian Massif. The 22 focal mechanism solutions are consistent with a strike-slip stress tensor with σ_1 trending N156° E and a σ_3 striking N066° E, with an R factor of 0.81 (Figure 5). The focal mechanisms for the main shock of each sequence are consistent with the regional stress tensor [Haessler and Hoang-Trong, 1988, Plenefisch and Bonjer, 1997, Got et al., 2011]. The migration of earthquakes during both the Remiremont and Rambervilliers sequences, but also over the whole 1964–1999 period [Audin et al., 2002], has been interpreted as the involvement of fluids, probably coming from the sedimentary cover, into the pre-fractured basement. The sporadic seismic activity has also been interpreted as due to the existence of barriers, due to mineral crystallization into the dense network of fractures dilated by fluids, as confirmed by the presence of a high conductivity anomaly evidenced by electrical resistivity measurements [Bourlange et al., 2012]. The main shocks induce the breaking of these barriers, which allows fluid migration along the pressure gradient through diffusion processes. Using the measured rate of the seismicity migration, an estimate of the permeability value of the fault zone has been proposed for the region [10^{-13}, 10^{-16} m^2; Audin et al., 2002] consistent with other observations of earthquake migration induced by fluids, such as at geothermal sites [Shapiro, 2000, Shapiro et al., 1999, Audigane et al., 2002].

7. Artois–Brabant–Hainaut–Ardennes

In this section we consider the broad area including the northern Paris Basin, the Artois, the Brabant Massif, the Ardennes Massif and the region of Maastricht. This zone can be divided into two major geological zones, the northern and eastern parts of the Paris Basin with extremely low seismicity and its northern peripheral regions (Ardennes, Brabant Massif, Artois) where seismicity is moderate but not negligible (Figure 10). The study of the seismicity of this region requires an interest in Belgian seismicity, part of which takes place close to the French border. As mentioned in the Data section, we complemented our data set with the historical and instrumental catalogues of the Royal Observatory of Belgium (www.seismologie.be). We note that most of the catalogue has been built from the French seismic monitoring network explaining the low number of low-magnitude seismicity revealed by the low b-value (1.06) for the whole area (Supplementary Figure 7f). Despite being the locus of one of the major earthquakes which occurred in western Europe (June 20, 1995 M_w = 4.1 epicenter at Roeulx and April 13, 1992 M_w = 5.3 epicenter at Roermond in the Netherlands, also called

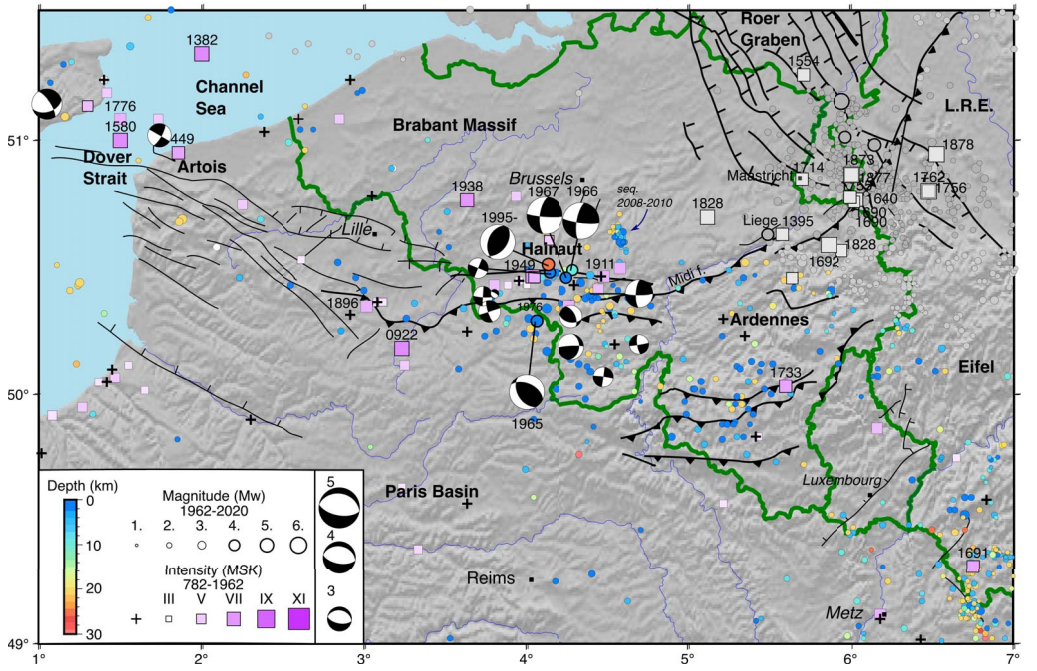

Figure 10. Seismic activity in the region of Northern France and Belgium (see location on Figure 1). The tectonic structures are from de Béthune and Bouckaert [1968], Camelbeeck et al. [2007] and García-Moreno et al. [2015].

Maastricht event), we do not focus on the eastern part of the Ardennes Massif, the Roer Graben and the Lower-Rhine Embayement, which are relatively far from Northeastern France, and for which specific seismologic, tectonic and geodetic studies have been made [e.g., Ahorner, 1975, 1985, 1996, Camelbeeck and Meghraoui, 1998, Meghraoui et al., 2000, Reamer and Hinzen, 2004, Hinzen and Reamer, 2007, Camelbeeck et al., 2007, Alexandre et al., 2008, Lecocq, 2011, Hinzen et al., 2021].

The seismicity in the Eifel province remains low, diffuse, and characterized by low-magnitude events [Ahorner, 1983]. This point should be mentioned in light of the recent results of surface deformation in this area, which is consistent with a dynamic uprise of the deep mantle below the volcanic field [Kreemer et al., 2020, Ritter et al., 2001, Dahm et al., 2020]. Using the local seismic network of the University of Cologne and relocation process, Hinzen et al. [2021] show that whereas seismicity is lacking where the surface uplift is the largest (~1 mm/yr), clusters of seismicity concentrate where gradients of vertical movements are measured. Peculiar events such as deep low frequency earthquakes have been identified and located from 10 to 40 km of depth revealing vertical paths of ascending magma [Hensch et al., 2019].

North of the Western Ardennes, the seismic activity in the province of Hainaut is mainly concentrated within the east–west-trending, 12 km wide Mons Basin, delimited to the south by the Midi fault. It consists of an accumulation of 300 m of thick Meso-Cenozoic sediments. Since 1900, several earthquakes have caused damage in this region, such as the ones that occurred on June 3, 1911 (I = V), and on April 3, 1949 in Havré (I = VII). A series of three events occurred in the three consecutive years 1965 (M_w 4.3+), 1966 [M_w 4.6; Delouis et al., 1993], and 1967 [M_w 4.6; intensity VII; Camelbeeck et al., 2014]. Overall, the seismicity from 1965 to 1971 forms a sequence along the axis of the Mons Basin, dominated by strike-slip mechanisms. These events that take place in the coal mining areas are characterized by shallow focal depths (<2 km), suggesting their anthropogenic origin due to the mine exploitation at depth. The seismic activity in this region is attested since 1887, after the beginning of large-scale mining operations. Mining activity stopped around 1970. The last sequence

is concomitant with the end of mining, and only a few events were recorded afterward, such as the 1976 event (24 October, M_w = 3.5 I_{max} VI) whose shallow focal depth (2 km) also suggests a mining origin (Figure 10). However the Roeulx 1995 earthquake (20 June 20, M_w 3.4; Ml 4.5) is located slightly north of the Mons Basin and differs from the previous sequence since its hypocentral depth is of ∼25 km and its focal mechanism corresponds to a reverse fault. Among 20 focal mechanisms the stress inversion includes 19 fault planes and obtains a σ_1 trending N115° E and a σ_2 striking N025° E, with an R factor of 0.25 (Figure 5). The stress tensor illustrates the WNW–ESE compression crustal deformation in agreement with the tectonic background of the Ardennes Massif. The only recent activity to be noted are the few earthquakes in the region situated south of the Midi fault between 1992 and 2010 (Figure 10). With a magnitude M_w ranging from 1.5 to 3.2, they are located in a region that has seen the impoundment of water by several dams over this period, but they are not located exactly under the lakes. The link between seismicity and dams, though it can be considered, has not been demonstrated.

The Brabant Massif located at the north of the Hainaut province (Figure 10), is affected by low seismicity. However, the earthquake of 1828 (23 February) is one of the largest events in this intraplate region (I_{max} = VI to VII). The damage was significant and the effects were felt up to 100 km away, with spatial variations related to the role of the sedimentary cover on the shaking taken into account when estimating the parameters of the focal source from historical documents [Camelbeeck et al., 2021]. More recently, the earthquake of 11 June 1938 in Belgium (M_w 5.4 I_{max} VII) is the most important localized event of the twentieth century in this area. Its depth of 20–30 km suggests that it could be linked to faults in the basement, but not to an active structure on the surface. Located south of Ghent on the border between Flanders and Wallonia, it is often called the Audenarde earthquake. This earthquake was followed by six aftershocks coming from the same locus as the main shock (the differences in time between the P and S waves were the same for all the events). Two of these aftershocks reached the magnitude M_w 4.0 and were strongly felt in the epicentral zone.

Another sequence occurred in the Brabant Massif between 2008 and 2010, southeast of Brussels (Figure 10). The earthquakes were of magnitude M_w between −0.9 and 3.2 and concentrated within an area of small dimension (<10 × 10 km^2). The hypocentral distribution (depth ranging from 5.5 to 7 km) draws a fault surface that coincides with an ancient NW-SE structure in the basement determined by gravimetry [Van Noten et al., 2015]. It is likely that on this same structure a sequence of earthquakes with magnitude (ML) up to 4 took place in the 1950s, a sequence that is unfortunately poorly documented due to a lack of instrumental data.

The last notable area of study includes the Artois region and the Channel Sea region. It is characterized by low micro-seismic activity probably due to the relatively high detection threshold of the seismic network in this region, but also due to the occurrence of large events. In the Artois region, the most significant known event occurred in 1896 [2 June, with an intensity VI; Manchuel et al., 2018]. It is likely that this earthquake occurred on tectonic structures; however, the question of the link between mining activity in the Pas-de-Calais and this earthquake arises in a region known to have had little seismic activity before the development of the mines. On the industrial side, Belgian and French geologists denied, at the time, any responsibility for the occurrence of this earthquake.

At the extreme west of the region under study, several historical earthquakes were observed in the Dover Strait in 1382 (I = VII–VIII), 1580 (I = VII–VIII) and 1776 (I = VI), [Melville et al., 1996]. The most important one, that of 6 April 1580, has a maximum intensity of VIII and an estimated magnitude of M_w ∼ 5.8–6.0. All these earthquakes likely took place closer to the English than the French coastlines, probably on Variscan tectonic accidents of the North Artois shear zone, suggesting the seismogenic potential of these faults [Melville et al., 1996, Camelbeeck et al., 2007]. From recent analysis of bathymetric and seismic data, García-Moreno et al. [2015] identified a broad structural zone comprising several subparallel WNW–ESE trending faults and folds, an indication of possible Quaternary fault activity. They nevertheless have a strong destructive potential on the French territory, as illustrated dramatically by the destruction of fortifications and buildings in Calais and Lille in 1580. This may suggest a link between these earthquakes and sea level variations in the Channel and the North Sea; however the effects of the end of

the glaciation and the related strong variations in sea level probably no longer exist at the present time.

8. Discussion

In order to investigate the seismic activity of northeastern France and surrounding areas and its implications for the seismic hazard assessment for the region, three main issues still need to be addressed: (1) What are the origins of the current intraplate earthquakes and what is the significance of the low-magnitude seismicity? (2) Is the occurrence of a large earthquake (with magnitude >7 on the identified active faults) with a long recurrence interval a possible scenario? (3) Can we consider the notion of seismic cycle for the faults located in this low strain rate domain? We have shown in previous sections that the earthquake activity in the study region is not of high level, but that it is likely to be associated with some seismic hazard and risk. This is to be taken into account, particularly in view of the presence of large urban areas, industrial (chemical factories, nuclear power plants) and other environmentally sensitive facilities in the densely populated western Europe.

8.1. *Various origins and significance of the intraplate seismicity*

This review of the seismic activity in northeastern France and adjacent areas points out that the seismicity recorded within each region mainly occurs on or around pre-existing tectonic structures. However, the space–time evolution of the seismic activity seems to be specific to each region. The URG is affected by a seismic activity mainly related to the faults associated with the rift formation, either bordering or located within the central graben. More paleoseismic and tectonic constraints are necessary both to identify the potentially active faults and to describe their behavior and their Quaternary and present-day history. A closer look at the seismicity reveals that the activity in the N- and S-URG can be characterized by a regular "background seismicity" superimposed by sequences limited in space and time. The seismicity in Jura forelands and the external range is mainly diffuse in this wide region, without the occurrence of many sequences, challenging a clear attribution of these ruptures to individual structures such as the thrusts of the chain propagating northwards or the normal or strike-slip faults of the Rhone–Rhine transfer zone. Conversely, the numerous sequences occurring in the western Vosges reveal epicenter alignments consistent with known ancient structures in the crystalline massif. However they have been primarily interpreted as the presence of fluids diffusing into a pre-fractured medium. Therefore, with or without the involvement of fluids, most of the background seismicity or the specific sequences are of tectonic origin in an intraplate context, i.e. where the strain rates remain low.

However, the low level of seismic rate, the low magnitudes, and in particular the sparsity of moderate events with their related aftershock sequence also reveal the relative importance of non-tectonic events. Anthropogenic seismicity has been observed in almost all the considered sub-regions of our study. In the URG, we mentioned the seismicity induced by the geothermal industry, in particular in the region of Basel, Strasbourg, in northern Alsace and in southern Rhineland–Palatinate (Germany, Figure 1). Because the trigger is primarily the injection tests at depth, this seismicity occurs mainly through sequences of micro-events sometimes accompanied with larger events. Finally, the region has also been largely affected by mine-induced seismicity, in the Lorraine Plateau, in Saar and Ardennes. Low-magnitude events probably occurred as in S-URG as well, at the location of the Mines de Potasse d'Alsace, whereas large events and significant events have been observed in Hainaut region. Other sources can be mentioned, such as the filling/infilling of dams (south of Hainaut).

This human-induced seismic activity has two implications. First, the analysis of the natural seismotectonics of this intraplate domain requires considering the non-negligible number of anthropogenic seismic sources in order to better understand the origin and behavior of the tectonic-related seismicity of the region. This implies that a solid step of discrimination has to be implemented in the building of seismic catalogues. Traditionally made by hand by analysts, in the seismic monitoring observatory, this step now benefits from the recent methodological developments that have been made using artificial intelligence/machine learning, etc. Second, as shown earlier, the region under study is regularly affected by natural seismic sequences or even moderate earthquakes which occur on pre-existing structures, in-

dicating that these have been loaded at a very-low strain rate. Therefore, as suggested by the ongoing 2019–2021 crisis north of Strasbourg, the region has a seismogenic potential and the seismic hazard increases with anthropogenic activities which influences the state of a loaded seismogenic fault plane by either changing its properties or perturbing the stress state.

Even though the current seismic catalogues in an intraplate domain represent rare and valuable data sets to investigate the seismic hazard of a given region, the spatial pattern of low-magnitude earthquakes does not necessarily reflect past and future activity, as underlined by Camelbeeck et al. [2007]. However, in northeastern France, the historical and instrumental catalogues are quite consistent for most of the sub-regions, except in the N-URG where many historical earthquakes have been reported and very few remarkable events are present in the instrumental catalogue (see below). All of the sub-regions are characterized by large networks of pre-existing faults but the knowledge of their recent activity suffers from the lack of quantitative constraints. The current network and the accuracy of the hypocentral locations do not allow us to reduce our scale of observation and identify fault planes from the hypocentral space distribution. However, the set of focal mechanisms indicates a strike-slip dominated stress regime, quite homogeneous over the whole region, in agreement with other stress databases [Heidbach et al., 2010, Zoback, 1992] or local inversions of focal mechanisms. The set of associated mechanisms and tensor results data show a predominance of σ_1 horizontal direction NNW–SSE to NW–SE, and strike-slip fault kinematics. Considering the significant observed normal faulting that limit the graben [Shipton et al., 2016], we suggest that a permutation of the principal stress axes of σ_1 and σ_2 can occur. With σ_3 horizontal, a vertical σ_1 (instead of σ_2) would favor extensional tectonics in line with the Quaternary crustal deformation observed along the URG. However, the stress tensor for each region is obtained from focal mechanisms of earthquakes with magnitudes between $1 < M_w < 4$ that favor strike-slip fault kinematics. These results may significantly change when earthquake magnitudes exceed M_w 5 where focal mechanisms and size of earthquake ruptures provide a better representation of the crustal deformation [Jackson and White, 1989, Stein et al., 2015]. The 22 February 2003 main shock earthquake in Rambervilliers (M_w 5.3; Vosges) presents normal faulting mechanisms (Figure 4) in contrast to strike-slip focal mechanisms for most of their aftershocks. This has been also observed for the 13 April 1992 main shock earthquake in Roermond (M_w 5.3; Lower-Rhine Graben).

As in other intraplate domains, the lack of detectable surface deformation associated with the loading of most of the pre-existing structures and the occurrence of transient events prevent the apprehending of the current seismic activity as the release of elastic strain accumulation. Our review sheds light on a "unique" stress regime for most of the subregions, although they are all characterized by distinct seismic behavior. Therefore, future investigations are necessary to better understand the significance of this background low-magnitude seismicity, and more specifically the mechanisms involved in the ruptures.

8.2. *Constraints on the long-term earthquake activity*

Three recurrence models of large earthquakes may be taken into consideration for seismogenic faults in regions of low strain rates: (1) *quasi-periodic*, as seen along fast active faults [e.g., Ambraseys, 1970, Sieh and Williams, 1990]; (2) *episodic activity* with 2–3 events separated by approximately 10^3 years or relatively long periods of quiescence over 3×10^3 to 10^4 years, as proposed for the stable continental regions like the central United States and Australia [Coppersmith, 1988, Crone and Luza, 1990, Crone, 1992]; (3) *Chaotic*, in case the whole brittle layer is mechanically strong without significant weaknesses, such that any pre-existing fault that is well-oriented with respect to the maximum horizontal stress would be potentially seismogenic. This last model is typically Poissonian in spatial and temporal occurrence; nevertheless, considering earthquake catalogues and paleoseismic results, it is highly unlikely that it applies to the western European seismotectonics.

Recent works have shown evidence of neotectonics and active faults capable of producing large earthquakes in intraplate Europe and have addressed the problem of coseismic surface ruptures and their return period [Camelbeeck and Meghraoui, 1998, Lemeille et al., 1999, Meghraoui et al., 2001, Van Noten et al., 2015, Shipton et al., 2016]. This

problem is fundamental in two different aspects: (1) if large earthquakes are preserved in the geologic record, they might be retrieved by detailed paleoseismic investigations, and (2) the study of active faults with visible surface ruptures in stable continental Europe is a significant step in the understanding of seismotectonic processes and earthquake generation [Stein et al., 2012]. A reappraisal of the seismic hazard should take into account the characteristics of earthquake faults in these regions of continental Europe.

Instrumental and historical earthquakes in the whole region have apparently not been large enough to cause surface rupturing. However, in the URG, the seismogenic layer reaches 20 km depth and observed fault segment lengths sometimes exceed 20 km, implying a moment magnitude $M_w > 6.5$ [Leonard, 2010]. Similarly, in the Roer Graben where the seismogenic layer is ~17 km thick, dimensions (~10 km long) and geometry of the faults derived from paleoseismic results would imply that moment magnitudes of earthquake could reach $M_w = 6.3$ [Jackson and White, 1989, Camelbeeck and Van Eck, 1994]. However, other fault segments along the graben may exceed 20 km in length, and may represent a potential for a M_w 6.6 or larger earthquake [Camelbeeck and Meghraoui, 1998].

It is mostly agreed that any late Quaternary tectonic activity in the URG is controlled by pre-existing faults in the area. Thus the study of cumulative subsurface deformation and related active faulting over a longer period is critical for a better understanding of the earthquake faulting and hazards. Paleoseismic results show that return periods for earthquakes similar to the 1356 Basel event (M_w 6.5) are of the order of 2500 years in the southern URG [Ferry et al., 2005], or of the order of 10,000 years in the LRG [Camelbeeck and Meghraoui, 1998]. Considering that reliable historical seismic records may not date back to more than 1000 years (if at all), this implies that other undocumented large earthquakes in the region may be missing in the seismicity catalogue; such large seismic events pose the problem of the identification of earthquake faulting and their long-term/short-term behavior.

9. Conclusion

The seismicity and seismotectonics of NE France and neighboring regions are investigated using the seismic catalogues of France (FCAT, Si-Hex, SisFrance), the mapped Quaternary and recently identified active faults. Our study addresses the seismotectonic characteristics of this intraplate domain that includes different tectonic zones such as the NW Jura, the southern and northern URG, the Vosges Mountains, and the Hainaut–Brabant–Artois regions. Moment magnitudes are considered for instrumental earthquakes (post-1962) and intensity scale MKS for historical earthquakes (pre-1962), providing a comprehensive picture of the most seismically active zones, obtained through a detailed analysis of seismicity rate. The seismicity distribution indicates the S-URG as the site of the most frequent earthquakes in the study region.

A synthesis of previous works in neotectonics and active tectonics and fault mapping mainly in the URG and Ardennes Massif is undertaken, and a stress tensor inversion of focal mechanisms is presented for each region. The stress field distribution and fault kinematics are in agreement with the previously studied stress distribution in Europe. However, the regional analysis of focal mechanisms reveals an interesting distribution of focal mechanisms and long-term crustal deformation associated with active strike-slip and normal faults in the URG, and thrust faults in the Ardennes Massifs. The existence of compressive geological structures (Ardennes) near a strike-slip/extension deformation system (URG) in the intraplate domain illustrates the complex intraplate tectonic movement in western Europe. The low seismic and geodetic strain rate obtained from seismicity and GNSS measurements strongly indicates that a proper understanding of the crustal deformation in these regions requires longer periods of observations and data collection. Further investigations in the identification of active faults, paleoseismology along with earthquake monitoring are needed in order to better understand the earthquake generation in NE France.

Acknowledgments

We deeply thank all the persons involved in the development of the French seismic monitoring network in northeastern France, especially Hervé Blumentritt, Hervé Wodling and Céleste Broucke (EOST). This paper is dedicated to Jacky Sahr who was very

active on these instrumental developments and regrettably passed away this year. We acknowledge Thierry Camelbeeck and Thomas Lecoq for data sharing and fruitful discussions, and an anonymous reviewer for his/her valuable comments on the manuscript. Data from the AlpArray Seismic Network have been collected with the help of the AlpArray Working Group, the list of members can be found at http://www.alparray.ethz.ch/en/seismic_network/backbone/data-policy-and-citation/.

Supplementary data

Supporting information for this article is available on the journal's website under https://doi.org/10.5802/crgeos.80 or from the author.

References

Ahorner, L. (1975). Present-day stress field and seismotectonic block move-ments along major fault zones in central Europe. *Tectonophysics*, 29, 233–249.

Ahorner, L. (1983). Historical seismicity and present-day activity of the Rhenish Massif, central Europe. In Fuchs, K., von Gehlen, K., Mälzer, H., Murawski, H., and Semmel, A., editors, *Plateau Uplift, the Rhenish Shield—A Case History*, pages 198–221. Springer-Verlag, Berlin.

Ahorner, L. (1985). The general pattern of seismotectonic dislocations in central Europe as the background for the Liège earthquake on November 8, 1983. In Melchior, P., editor, *Seismic Activity*, pages 41–56. D. Reidel Publishing Company, Western Europe: Dordrecht.

Ahorner, L. (1996). How reliable are speculations about large paleo-earthquakes at the western border fault of the Roer valley graben near Bree. In Bonatz, M., editor, *Comptes-Rendus des 81^{ièmes} Journées Luxembourgeoises de Géodynamique*, pages 39–57. Grand Duchy of Luxemburg, Walferdange.

Alexandre, P., Kusman, D., Petermans, T., and Camelbeeck, T. (2008). The 18 September 1692 Earthquake in the Belgian Ardenne and Its Aftershocks. In Fréchet, J., Meghraoui, M., and Stucchi, M., editors, *Historical Seismology*, volume 2 of *Modern Approaches in Solid Earth Sciences*. Springer, Dordrecht.

AlpArray Seismic Network (2015). AlpArray Seismic Network (AASN) temporary component. AlpArray Working Group. Other/Seismic Network; Datacite Link: http://data.datacite.org/10.12686/alparray/z3_2015.

Ambraseys, N. M. (1970). Some characters features of the Anatolian fault zone. *Tectonophysics*, 9, 143–165.

Audigane, P., Royer, J.-J., and Kaieda, H. (2002). Permeability characterization of the Soultz and Ogachi large-scale reservoir using induced microseismicity. *Geophys.*, 67, 204–211.

Audin, L., Avouac, J. P., Flouzat, M., and Plantet, J. L. (2002). Fluid-driven seismicity in a stable tectonic context: The Remiremont fault zone, Vosges, France. *Geophys. Res. Lett.*, 29(6).

Baize, S., Cushing, M., Lemeille, F., and Jomard, E. (2013). Updated seismotectonic zoning scheme of Metropolitan France, with reference to geologic and seismotectonic data. *Bull. Soc. Géol. Fr.*, 184, 225–259.

Bano, M., Edel, J.-B., Herquel, G., and EPGS Class 2001–2002 (2002). Geophysical investigation of a recent shallow fault. *Lead. Edge*, 21, 648–650.

Barth, A., Ritter, J. R. R., and Wenzel, F. (2015). Spatial variations of earthquake occurrence and coseismic deformation in the Upper Rhine Graben, Central Europe. *Tectonophysics*, 651–652, 172–185.

Becker, A. (2000). The Jura Mountains: An active foreland fold-and-thrust belt? *Tectonophysics*, 32, 381–406.

Behrmann, J. H., Hermann, O., Horstmann, M., Tanner, D. C., and Bertrand, G. (2003). Anatomy and kinematics of oblique continental rifting revealed: A three-dimensional case study of the southeast Upper Rhine graben (Germany). *AAPG Bull.*, 87, 1105–1121.

Bertrand, D., Elsass, P., Wirsing, G., and Luz, A. (2006). Quaternary faulting in the Upper Rhine Graben revealed by high-resolution multi-channel reflection seismic. *C. R. Géosci.*, 338, 574–580.

Bogusz, J., Klos, A., and Pokonieczny, K. (2019). Optimal strategy of a GPS position time series analysis for post-glacial rebound investigation in Europe. *Remote Sens.*, 11, article no. 1209.

Bonjer, K.-P. (1997). Seismicity pattern and style of seismic faulting at the eastern border fault of the southern Rhine Graben. *Tectonophysics*, 275, 41–69.

Bourlange, S., Mekkawi, M., Conin, M., and Schnegg, P.-A. (2012). Magnetotelluric study of the Remiremont-Epinal-Rambervillers zone of migrating seismicity, Vosges (France). *Bull. Soc. Géol. Fr.*, 183, 461–470.

Brun, J.-P. and Gutscher, M.-A. (1992). DEKORP-ECORS teams, Deep crustal structure of the Rhine Graben from DEKORP-ECORS seismic reflection data: A summary. *Tectonophysics*, 208, 139–147.

Calais, E., Camelbeeck, T., Stein, S., Liu, M., and Craig, T. J. (2016). A new paradigm for large earthquakes in stable continental plate interiors. *Geophys. Res. Lett.*, 43, 10,621–10,637.

Camelbeeck, T., Alexandre, P., Sabbe, A., Knuts, E., Moreno, D., and Lecocq, T. (2014). The impact of the earthquake activity in Western Europe from the historical and architectural heritage records. In Talwani, P., editor, *Intraplate Earthquakes*, pages 198–230. Cambridge University Press.

Camelbeeck, T., Knuts, E., Alexandre, P., Lecocq, T., and Van Noten, K. (2021). The 23 February 1828 Belgian earthquake: a destructive moderate event typical of the seismic activity in Western Europe. *J. Seismol.*, 25, 369–391.

Camelbeeck, T. and Meghraoui, M. (1998). Geological and geophysical evidence for large paleoearthquakes with surface faulting in the Roer Graben (northwest Europe). *Geophys. J. Int.*, 132, 347–362.

Camelbeeck, T. and Van Eck, T. (1994). The Roer Valley graben earthquake of 13 April 1992 and its seismotectonic setting. *Terra Nova*, 6, 291–300.

Camelbeeck, T., Vanneste, K., et al. (2007). Relevance of active faulting and seismicity studies to assess longterm earthquake activity in Northwest Europe. In Stein, S. and Mazzotti, S., editors, *Continental Intraplate Earthquakes: Science, Hazard, and Policy Issues*, Geol. Soc. Am., Spec. Pap., 425, pages 193–224.

Cara, M., Brüstle, W., Gisler, M., Kästli, P., Sira, C., Weihermüller, C., and Lambert, J. (2005). Transfrontier macroseismic observations of the ML = 5.4 earthquake of February 22, 2003 at Rambervillers, France. *J. Seismol.*, 9, 317–328.

Cara, M., Cansi, Y., Schlupp, A., et al. (2015). SI-Hex: a new catalogue of instrumental seismicity for metropolitan France. *Bull. Soc. Géol. Fr.*, 186, 3–19.

Charléty, J., Cuenot, N., Dorbath, L., Dorbath, C., Haessler, H., and Frogneux, M. (2007). Large earthquakes during hydraulic stimulations at the geothermal site of Soultz-sous-Forêts. *Int. J. Rock Mech. Mining Sci.*, 44, 1091–1105.

Chartier, T., Scotti, O., Clément, C., Jomard, H., and Baize, S. (2017). Transposing an active fault database into a fault-based seismic hazard assessment for nuclear facilities — Part 2: Impact of fault parameter uncertainties on a site-specific PSHA exercise in the Upper Rhine Graben, eastern France. *Nat. Hazards Earth Syst. Sci.*, 17, 1585–1593.

Chauve, P., Martin, J., Petitjean, E., and Sequeiros, F. (1988). Le chevauchement du Jura sur la Bresse; données nouvelles et ré-interprétation des sondages. *Bull. Soc. Géol. Fr.*, IV(5), 861–870.

Coppersmith, K. J. (1988). Temporel and spatial clustering of earthquake activity in the Central and eastern United States. *Seismol. Res. Lett.*, 59, 299–304.

Cornou, C. et al. (2021). Rapid response to the M_w 4.9 earthquake of November 11, 2019 in Le Teil, Lower Rhône Valley, France. *C. R. Géosci.* this issue.

Crone, A. J. (1992). Structural relations and earthquake hazards of the Crittenden County fault zone, northeastern Arkansas. *Seismol. Res. Lett.*, 63, 249–262.

Crone, A. J. and Luza, K. V. (1990). Style and timing of Holocene surface faulting on the Meers fault, southwestern Oklahoma. *Geol. Soc. Am. Bull.*, 102, 1–17.

Dahm, T., Stiller, M., Mechie, J., Heimann, S., Hensch, M., Woith, H., et al. (2020). Seismological and geophysical signatures of the deep crustal magma systems of the Cenozoic volcanic fields beneath the Eifel, Germany. *Geochem. Geophys. Geosyst.*, 21, article no. e2020GC009062.

de Béthune, P. and Bouckaert, L. (1968). Geological Map of Belgium and Neighbouring Countries: Brussels, Geological survey of Belgium Miscellaneous Geological Maps, scale 1:2,000,000, 1 sheet.

Deichmann, N. (1992). Structural and rheological implications of lower-crustal earthquakes below northern Switzerland. *Phys. Earth Planet. Inter.*, 69, 270–280.

Deichmann, N., Kraft, T., and Evans, K. F. (2014). Identification of faults activated during the stimulation of the Basel geothermal project from cluster analysis and focal mechanisms of the larger magnitude events. *Geothermics*, 52, 84–97.

Delacou, B., Sue, C., Champagnac, J.-D., and

Burkhard, M. (2004). Present-day geodynamics in the bend of the western and central Alps as constrained by earthquake analysis. *Geophys. J. Int.*, 158, 753–774.

Delacou, B., Sue, C., Nocquet, J.-M., Champagnac, J.-D., Allanic, C., and Burkhard, M. (2008). Quantification of strain rate in the Western Alps using geodesy: comparisons with seismotectonics. *Swiss J. Geosci.*, 101, 377–385.

Delouis, B., Haessler, H., Cisternas, A., and Rivera, L. (1993). Stress tensor determination in France and neighbouring regions. *Tectonophysics*, 221, 413–438.

Delvaux, D. and Sperner, B. (2003). New aspects of tectonic stress inversion with reference to the TENSOR program. In Nieuwland, D., editor, *New Insights into Structural Interpretation and Modelling*, volume 212, pages 75–100. Geological Society Special Publication, London.

Dèzes, P., Schmid, S. M., and Ziegler, P. A. (2004). Evolution of the European Cenozoic Rift System: Interaction of the Alpine and Pyrenean orogens with their foreland lithosphere. *Tectonophysics*, 389, 1–33.

Doebl, F. (1970). Die tertiären und quartären Sedimente des südlichen Rheingrabens. In Illies, J. H. and Mueller, S., editors, *Graben Poblem. Proceedings of an International Rift Symposium held in Karlsruhe October 10–12, 1968*, pages 56–66, Stuttgart. E. Schweizerbart'sche.

Dorbath, L., Cuenot, N., Genter, A., and Frogneux, M. (2009). Seismic response of the fractured and faulted granite of Soultz-sous-Forêts (France) to 5 km deep massive water injections. *Geophys. J. Int.*, 177, 653–675.

Ebel, J. E., Bonjer, K.-P., and Oncescu, C. M. (2000). Paleoseismicity: Seismicity evidence for past large earthquakes. *Seismol. Res. Lett.*, 71, 283–294.

Fäh, D., Gisler, M., Jaggi, B., Kästli, B., Lutz, T., Masciadrt, V., Matt, C., Mayer-Rosa, D., Rippmann, D., Schwarz-Zanetti, G., Tauber, J., and Wenk, T. (2009). The 1356 Basel earthquake: an interdisciplinary revision. *Geophys. J. Int.*, 178, 351–374.

Federal Institute for Geosciences and Natural Resources (1976). German Regional Seismic Network (GRSN). Bundesanstalt für Geowissenschaften und Rohstoffe.

Ferry, M., Meghraoui, M., Delouis, B., and Giardini, D. (2005). Evidence for Holocene paleoseismicity along the Basel–Reinach active normal fault (Switzerland): a seismic source for the 1356 earthquake in the Upper Rhine graben. *Geophys. J. Int.*, 158, 1–21.

Ford, M., Le Carlier de Veslud, C., and Bourgeois, O. (2007). Kinematic and geometric analysis of fault-related folds in a rift setting: the Dannemarie basin, Upper Rhine Graben. *J. Struct. Geol.*, 29, 1811–1830.

Fracassi, U., Nivière, B., and Winter, T. (2005). First appraisal to define prospective seismogenic sources from historical earthquakes damages in southern Upper Rhine Graben. *Quat. Sci. Rev.*, 24, 401–423.

Fuhrmann, T., Caro Cuenca, M., Knöpfler, A., van Leijen, F. J., Mayer, M., Westerhaus, M., Hanssen, R. F., and Heck, B. (2015). Estimation of small surface displacements in the Upper Rhine Graben area from a combined analysis of PS-InSAR, levelling and GNSS data. *Geophys. J. Int.*, 203, 614–631.

Fuhrmann, T., Heck, B., Knöpfler, A., Masson, F., Mayer, M., Ulrich, P., Westerhaus, M., and Zippelt, K. (2013). Recent surface displacements in the Upper Rhine Graben – Preliminary results from geodetic networks. *Tectonophysics*, 602, 300–315.

García-Moreno, D., Verbeeck, K., Camelbeeck, T., De Batist, M., Oggioni, F., Zurita Hurtado, O., Versteeg, W., Jomard, H., Collier, J. S., Gupta, S., Trentesaux, A., and Vanneste, K. (2015). Fault activity in the epicentral area of the 1580 Dover Strait (*Pas-de-Calais*) earthquake (northwestern Europe). *Geophys. J. Int.*, 201, 528–542.

Gephart, J. W. and Forsyth, D. W. (1984). An improved method for determining the regional stress tensor using earthquake focal mechanism data — application to the San-Fernando earthquake sequence. *J. Geophys. Res.*, 89, 9305–9320.

Giamboni, M., Wetzel, A., Nivière, B., and Schumacher, M. (2004). Plio-Pleistocene folding in the southern Rhinegraben recorded by the evolution of the drainage network (Sundgau area; northwestern Switzerland and France). *Eclogae Geol. Helv.*, 97, 17–31.

Got, J.-L., Monteiller, V., Guilbert, J., Marsan, D., Cansi, Y., Maillard, C., and Santoire, J.-P. (2011). Strain localization and fluid migration from earthquake relocation and seismicity analysis in the western Vosges (France). *Geophys. J. Int.*, 185, 365–384.

Haessler, H. and Hoang-Trong, P. (1988). La crise sismique de Remiremont (Vosges) de décembre 1984: implications tectoniques régionales. *C. R. Acad. Sci. Paris*, 300, 671–675.

Häge, M. and Joswig, M. (2009). Spatiotemporal distribution of aftershocks of the 2004 December 5 M_L = 5.4 Waldkirch (Germany) earthquake. *Geophys. J. Int.*, 178, 1523–1532.

Haimberger, R., Hoppe, A., and Schäfer, A. (2005). High-resolution seismic survey on the Rhine River in the northern Upper Rhine Graben. *Int. J. Earth Sci.*, 94, 657–668.

Heidbach, O., Tingay, M., Barth, A., Reinecker, J., Kurfeß, D., and Muller, B. (2010). Global crustal stress pattern based on the world stress map database release 2008. *Tectonophysics*, 482, 3–15.

Henrion, E., Masson, F., Doubre, C., Ulrich, P., and Meghraoui, M. (2020). Present-day deformation in the Upper Rhine Graben from GNSS data. *Geophys. J. Int.*, 223, 599–611.

Hensch, M., Dahm, T., Ritter, J., Heimann, S., Schmidt, S., Stange, S., and Lehmann, K. (2019). Deep low-frequency earthquakes reveal ongoing magmatic recharge beneath Laacher See Volcano (Eifel, Germany). *Geophys. J. Int.*, 216, 2025–2036.

Hinzen, K.-G. and Reamer, S. (2007). Seismicity, seismotectonics, and seismic hazard in the Northern Rhine Area. In *Continental Intraplate Earthquakes: Science, Hazard, and Policy Issues*, Geol. Soc. Am., Spec. Pap., 425, pages 225–242.

Hinzen, K. G., Reamer, S. K., and Fleischer, C. (2021). Seismicity in the Northern Rhine Area (1995–2018). *J. Seismol.*, 25, 351–367.

Houlié, N., Woessner, J., Giardini, D., et al. (2018). Lithosphere strain rate and stress field orientations near the Alpine arc in Switzerland. *Sci. Rep.*, 8.

Illies, J. H. (1981). Mechanism of graben formation. *Tectonophysics*, 73, 249–266.

Illies, J. H. and Greiner, G. (1979). Holocene movements and state of stress in the Rhine Graben rift system. *Tectonophysics*, 52, 349–359.

Institut de Physique du Globe de Paris (IPGP) and Ecole et Observatoire des Sciences de la Terre de Strasbourg (EOST) (1982). GEOSCOPE, French Global Network of broadband seismic stations. Institut de Physique du Globe de Paris (IPGP).

Jackson, J. and White, N. J. (1989). Normal faulting in the upper continental crust : observations from regions of active extension. *J. Struct. Geol.*, 11, 15–36.

Jomard, H., Cushing, E. M., Palumbo, L., Baize, S., David, C., and Chartier, T. (2017). Transposing an active fault database into a seismic hazard fault model for nuclear facilities – Part 1: Building a database of potentially active faults (BDFA) for metropolitan France. *Nat. Hazards Earth Syst. Sci.*, 17, 1573–1584.

Jouanne, F., Menard, G., and Darmendrail, X. (1995). Present-day vertical displacements in the northwestern Alps and southern Jura Mountains—Data from leveling comparisons. *Tectonics*, 14, 606–616.

Kappelmeyer, O., Gérard, A., Schloemer, W., Ferrandes, R., Rummel, F., and Benderitter, Y. (1991). European HDR project at Soultz-sous-Forêts, general presentation. *Geotherm. Sci. Technol.*, 2, 163–189.

Kastrup, U., Zoback, M. L., Deichmann, N., Evans, K., and Giardini, D. (2004). Stress field variations in the Swiss Alps and the northern Alpine foreland. *J. Geophys. Res.*, 109.

Kervyn, F., Ferry, M., Alasset, P. J., Jacques, E., and Meghraoui, M. (2002). The potential for a large earthquake in intraplate Europe: The contribution of remote sensing. In *EGS Meeting with Abstract (Poster), Nice, France*.

Kostrov, B. (1974). Seismic moment and energy of earthquakes and seismic flow of rock. *Izv. Acad. Sci. USSR, Phys. Solid Earth*, 1, 23–40.

Kraft, T. and Deichmann, N. (2014). High-precision relocation and focal mechanism of the injection-induced seismicity at the Basel EGS. *Geothermics*, 52, 59–73.

Kreemer, C., Blewis, G., and Davis, P. M. (2020). Geodetic evidence for a buoyant mantle plume beneath the Eifel volcanic area, NW Europe. *Geophys. J. Int.*, 222, 1316–1332.

Lacombe, O. and Mouthereau, F. (2002). Basement-involved shortening and deep detachment tectonics in forelands of orogens: Insights from recent collision belts (Taiwan, Western Alps, Pyrenees). *Tectonics*, 21, article no. 1030.

Lambert, J., Winter, T., Dewez, T. J. B., and Sabourault, P. (2005). New hypotheses on the maximum damage area of the 1356 Basel earthquake (Switzerland). *Quat. Sci. Rev.*, 24, 383–401.

Landesamt Für Geologie, Rohstoffe Und Bergbau (2009). Landeserdbebendienst Baden-Wuerttemberg [Data set]. International Federation of Digital Seismograph Networks.

https://doi.org/10.7914/SN/LE.

Lecocq, T. (2011). *L'activité sismique en Ardenne et sa relation avec la tectonique active*. PhD thesis, Université libre de Bruxelles, Belgium. 265 p. Unpublished.

Lemeille, F., Cushing, M. E., Cotton, F., et al. (1999). Evidence for Middle to Late Pleistocene faulting within the northern Upper Rhine Graben (Alsace Plain, France). *Earth Planet. Sci.*, 328, 839–846.

Leonard, M. (2010). Earthquake fault scaling: self-consistent relating of rupture length, width, average displacement, and moment release. *Bull. Seismol. Soc. Am.*, 100, 1971–1988.

Levret, A., Backe, J. C., and Cushing, M. (1994). Atlas of macroseismic maps for French earthquakes with their principal characteristics. *Nat. Hazards*, 10, 19–46.

Leydecker, G. (2009). *Earthquake Catalogue for the Federal Republic of Germany and Adjacent Areas for the Years 800–2002 — Datafile*. Federal Institute for Geosciences and Natural Resources, Hannover, Germany, http://www.bgr.de/quakecat.

Lopes Cardozo, G. and Behrmann, J. (2006). Kinematic analysis of the Upper Rhine graben boundary fault system. *J. Struct. Geol.*, 28, 1028–1039.

Lopes Cardozo, G., Edel, J.-B., and Granet, M. (2005). Detection of active crustal structures in the Upper Rhine graben using local earthquake tomography, gravimetry and reflection seismic. *Quat. Sci. Rev.*, 24, 339–346.

Madritsch, H., Fabbri, O., Hagedorn, E.-M., Preusser, F., Schmid, S. M., and Ziegler, P. A. (2010). Feedback between erosion and active deformation: Geomorphic constraints from the frontal Jura fold-and-thrust belt (eastern France). *Int. J. Earth Sci.*, 99, 103–122.

Madritsch, H., Kounov, A., Schmid, S. M., and Fabbri, O. (2009). Multiple fault reactivations within the intra-continental Rhine–Bresse Transfer Zone (La Serre Horst, eastern France). *Tectonophysics*, 471, 297–318.

Manchuel, K., Traversa, P., Baumont, D., Cara, M., Nayman, E., and Durouchoux, C. (2018). The French seismic CATalogue (FCAT-17). *Bull. Earthq. Eng.*, 16, 2227–2251.

Masson, C., Mazzotti, S., and Vernant, P. (2019). Precision of continuous GPS velocities from statistical analysis of synthetic time series. *Solid Earth*, 10, 329–342.

Masson, F., Auclair, S., Bertil, D., Grunberg, M., Hernandez, B., Lambotte, S., Mazet-Roux, G., Provost, L., Saurel, J.-M., Schlupp, A., et al. (2021). The transversal seismicity action RESIF: A tool to improve the distribution of the French seismicity products. *Seismol. Res. Lett.*, 92, 1623–1641.

Maury, J., Cornet, F., and Dorbath, L. (2013). A review of methods for deter- mining stress fields from earthquakes focal mechanisms; application to the Sierentz 1980 seismic crisis (upper Rhine Graben). *Bull. Soc. Géol. Fr.*, 184, 319–334.

Mayer-Rosa, D. and Cadiot, B. (1979). A review of the 1356 Basel earthquake: basic data. *Tectonophysics*, 53, 325–333.

Mazzotti, S., Aubagnac, C., Bollinger, L., Oscanoa, K., Delouis, B., Do Paco, D., Doubre, C., Godano, M., Jomard, H., Larroque, C., Laurendeau, A., Masson, F., Sylvander, M., and Trilla, A. (2021). FMHex20: An earthquake focal mechanism database for seismotectonic analyses in metropolitan France and bordering regions. *BSGF - Earth Sci. Bull.*, 192, article no. 10.

Mazzotti, S., Jomard, H., and Masson, F. (2020). Processes and deformation rates generating seismicity in metropolitan France and conterminous Western Europe. *BSGF*, 191, article no. 19.

Meghraoui, M., Camelbeeck, T., Vanneste, K., Brondeel, M., and Jongman, D. (2000). Active faulting and paleoseismology along the Bree fault zone (lower Rhine graben, Belgium). *J. Geophys. Res.*, 105, 13809–13841.

Meghraoui, M., Delouis, B., Ferry, M., Giardini, D., Huggenberger, P., Spottke, I., and Granet, M. (2001). Active normal faulting in the upper Rhine graben and paleoseismic identification of the 1356 Basel earthquake. *Science*, 293, 2070–2073.

Melville, C., Levret, A., Alexandre, P., Lambert, J., and Vogt, J. (1996). Historical seismicity of the Strait of Dover–Pas de Calais. *Terra Nova*, 8, 626–647.

Meyer, B., Lacassin, R., Brulhet, J., and Mouroux, B. (1994). The Basel 1356 earthquake: which fault produced it? *Terra Nova*, 6, 54–63.

Modeste, G., Doubre, C., and Masson, F. (2021). Time evolution of mining-related residual subsidence monitored over a 24-year period using InSAR in southern Alsace, France. *Int. J. Appl. Observ. Geoinfo.*, 102, article no. 102392.

Nivière, B., Bruestle, A., Bertrand, G., Carretier, S., Behrmann, J., and Gourry, J.-C. (2008). Active tec-

tonics of the southeastern Upper Rhine Graben, Freiburg area (Germany). *Quat. Sci. Rev.*, 27, 541–555.

Nivière, B., Giamboni, M., Innocent, C., and Winter, T. (2006). Kinematic evolution of a tectonic wedge above a flat-lying décollement: The Alpine Foreland at the interface between the Jura Mountains (northern Alps) and the upper Rhine graben. *Geology*, 34, 469–472.

Nivière, B. and Winter, T. (2000). Pleistocene northwards fold propagation of the Jura within the southern upper Rhine graben: Seismotectonic implications. *Glob. Planet. Change*, 27, 263–288.

Nocquet, J.-M. (2012). Present-day kinematics of the Mediterranean: A comprehensive overview of GPS results. *Tectonophysics*, 579, 220–242. Special issue: Orogenic processes and structural heritage in Alpine-type mountain belts.

Nocquet, J.-M., Sue, C., Walpersdorf, A., et al. (2016). Present-day uplift of the western Alps. *Sci. Rep.*, 6, article no. 28404.

Omori, F. (1894). Investigation of aftershocks. *Rep. Earthq. Inv. Comm.*, 2, 103–139.

Peltier, W. R., Argus, D. F., and Drummond, R. (2015). Space geodesy constrains ice age terminal deglaciation: the global ICE-6G C (VM5a) model. *J. Geophys. Res.*, 120, 450–487.

Perrey, A. (1844). Mémoire sur les tremblements de terre ressenties en France, Belgique et Hollande (depuis le 4ème siècle jusqu'à 1843). *Acad. Sci. de Belgique, t.*, XVIII, 1–110.

Peters, G., Buchmann, T. J., Connolly, P., van Balen, R. T., Wenzel, F., and Cloetingh, S. (2005). 521 Interplay between tectonic, fluvial and erosional processes along the Western Border Fault 522 of the northern Upper Rhine Graben, Germany. *Tectonophysics*, 406, 39–66.

Peters, G. and van Balen, R. T. (2007). Pleistocene tectonics inferred from fluvial terraces of the northern Upper Rhine Graben, Germany. *Tectonophysics*, 430, 41–65.

Piffner, O. A. (1990). Kinematics and intrabed-strain in mesoscopically folded limestone layers — Examples from the Jura and the helvetic zone of the Alps. *Eclogae Geol. Helv.*, 83, 585–602.

Plantet, J. L. and Cansi, Y. (1988). Accurate epicenters location with a large network example of the 1984/1985 Remiremont Sequence. In Bonin, J. et al., editors, *Seismic Hazard in Mediterranean Regions*, pages 347–358. Brussels and Luxemburg.

Plenefisch, T. and Bonjer, K.-P. (1997). The stress field in the Rhine graben area inferred from earthquake focal mechanisms and estimation of frictional parameters. *Tectonophysics*, 275(1–3), 71–97.

Rabin, M., Sue, C., Walpersdorf, A., Sakic, P., Albaric, J., and Fores, B. (2018). Present-day deformations of the Jura arc inferred by GPS surveying and earthquake focal mechanisms. *Tectonics*, 37, 3782–3804.

Reamer, S. K. and Hinzen, K.-G. (2004). An earthquake catalog for the northern Rhine Area, Central Europe (1975–2002). *Seismol. Res. Lett.*, 75, 713–725.

Renouard, A., Maggi, A., Grunberg, M., Doubre, C., and Hibert, C. (2021). Toward false event detection and quarry blast versus earthquake discrimination in an operational setting using semi-automated Machine Learning. *Seismol. Res. Lett.*

RESIF (1995a). RESIF-RAP French Accelerometric Network; RESIF - Réseau Sismologique et géodésique Français. http://dx.doi.org/10.15778/RESIF.RA.

RESIF (1995b). RESIF-RLBP French Broad-band Network, RESIF-RAP strong motion network and other seismic stations in metropolitan France; RESIF – Réseau Sismologique et géodésique Français. http://dx.doi.org/10.15778/RESIF.FR, RESIF, 2017.

RESIF (2017). RESIF-RENAG French National Geodetic Network, RESIF – Réseau Sismologique et géodésique Français. https://doi.org/10.15778/resif.rg.

Ritter, J. R., Jordan, M., Christensen, U. R., and Achauer, U. (2001). A mantle plume below the Eifel volcanic fields, Germany. *Earth Planet. Sci. Lett.*, 186, 7–14.

Rothé, J.-P. and Schneider, G. (1968). *Catalogue des tremblements de Terre du Fossé Rhénan.* Institut de Physique du Globe, Strasbourg. 91 p.

Rotstein, Y. and Schaming, M. (2008). Tectonic implications of faulting styles along a rift margin: The boundary between the Rhine Graben and the Vosges Mountains. *Tectonics*, 27, article no. TC2001.

Rotstein, Y., Schaming, M., and Rousse, S. (2005). Tertiary tectonics of the Dannemarie Basin, upper Rhine graben, and regional implications. *Int. J. Earth Sci. (Geol. Rundsch)*, 94, 669–679.

Rouland, D., Haessler, H., Bonjer, K., Gilg, B., Mayer-Raso, D., and Pavoni, N. (1983). The Sierentz Southern-Rhinegraben Earthquake of July 15,

1980. Preliminary results. *Dev. Solid Earth Geophys.*, 15, 441–446.

Royal Observatory Of Belgium (1985). Belgian Seismic Network [Data set]. International Federation of Digital Seismograph Networks. https://doi.org/10.7914/SN/BE.

Schmittbuhl, J., Lambotte, S., Lengliné, O., Grunberg, M., Jund, H., Vergne, J., Cornet, F., Doubre, C., and Masson, F. (2021). Induced and triggered seismicity below the city of Strasbourg, France from Nov 2019 to Jan 2021. *C. R. Géosci.* this issue.

Scotti, O., Baumont, D., Quenet, G., and Levret, A. (2004). The French macroseismic database SISFRANCE: objectives, results and perspectives. *Ann. Geophys.*, 47, 571–581.

Shapiro, S. (2000). An inversion for fluid transport properties in 3-D he- terogeneous rock using induced micro-seismicity. *Geophys. J. Int.*, 143, 931–936.

Shapiro, S., Audigane, P., and Royer, J. (1999). Large-scale in-situ permeabi- lity tensor of rocks from induced micro-seismicity. *Geophys. J. Int.*, 137, 207–213.

Shipton, Z. K., Meghraoui, M., and Monro, L. (2016). Seismic slip on the west flank of the Upper Rhine Graben (France-Germany): Evidence from tectonic morphology and cataclastic deformation bands. In Landgraf, A., Kuebler, S., Hintersberger, E., and Stein, S., editors, *Seismicity, Fault Rupture and Earthquake Hazards in Slowly Deforming Regions*, volume 432. Geological Society Special Publication, London.

Sieberg, A. (1940). Beitrage zum erdbebenkatalog Deutsch und angrenzendun jahr 58 bis 1799, Mitt. Deutsch Reichs-Erdebebend. *Haft*, 2, 112.

Sieh, K. E. and Williams, P. L. (1990). Behavior of the Southernmost San Andreas fault during the past 300 years. *J. Geophys. Res.*, 95, 6629–6645.

Sittler, C. (1985). Les Hydrocarbures d'Alsace dans le contexte historique et géodynamique du fossé Rhénan [The case history of oil occurrence in the Rhine Rift Valley]. *Bull. Cent. Rech. Explor. Prod. Elf-Aquitaine*, 9, 335–371.

Stein, S., Geller, R. J., and Liu, M. (2012). Why earthquake hazard maps often fail and what to do about it. *Tectonophysics*, 562–563, 1–25.

Stein, S., Liu, M., Camelbeeck, T., Merino, M., Landgraf, A., Hintersberger, E., and Kuebler, S. (2015). Challenges in assessing seismic hazard in intraplate Europe. In Landgraf, A., Kuebler, S., Hintersberger, E., and Stein, S., editors, *Seismicity, Fault Rupture and Earthquake Hazards in Slowly Deforming Regions*, volume 432. Geological Society Special Publication, London.

Sue, C. and Schmid, S. M. (2017). From ocean formation to mountain evolution in Alpine-type orogens. *Swiss J. Geosci.*, 110, 417–418.

Swiss Seismological Service (SED) at ETH Zurich (1983). National Seismic Networks of Switzerland. ETH Zürich. https://doi.org/10.12686/sed/networks/ch.

Sykes, L. R. (1978). Intraplate seismicity, reactivation of preexisting zones of weakness, alkaline magmatism, and other tectonism postdating continental fragmentation. *Rev. Geophys.*, 16, 621–688.

Thomas, J., Biermanns, P., Hürtgen, J., Reicherter, K., and Baize, S. (2017). Characterization of potentially active faults in the southern Upper Rhine Graben using GPR, 2017. In *9th International Workshop on Advanced Ground Penetrating Radar (IWAGPR)*, pages 1–6. https://doi.org/10.1109/IWAGPR.2017.7996047.

Thouvenot, F., Fréchet, J., Tapponnier, P., Thomas, J.-C., Le Brun, B., Ménard, G., Lacassin, R., Jenatton, L., Grasso, J.-R., Coutant, O., Paul, A., and Hatzfeld, D. (1998). The M_L 5.3 Epagny (French Alps) earthquake of 1996 July 15: a long-awaited event on the Vuache Fault. *Geophys. J. Int.*, 135, 876–892.

Trampert, J., Cara, M., and Frogneux, M. (1993). SH propagator matrix and Qs estimates from borehole- and surface-recorded earthquake data. *Geophys. J. Int.*, 112, 290–299.

Ustaszewski, K. and Schmid, S. M. (2006). Control of preexisting faults on geometry and kinematics in the northernmost part of the Jura fold-and-thrust belt. *Tectonics*, 25, article no. TC5003.

Ustaszewski, K. and Schmid, S. M. (2007). Latest Pliocene to recent thick-skinned tectonics at the Upper Rhine Graben – Jura Mountains junction. *Swiss J. Geosci.*, 100, 293–312.

Utsu, T. (1961). A statistical study on the occurrence of aftershocks. *Geophys. Mag.*, 30, 521–605.

Van Noten, K., Lecocq, T., Shah, A. K., and Camelbeeck, T. (2015). PSeismotectonic significance of the 2008–2010 Walloon Brabant seismic swarm in the Brabant Massif, Belgium. *Tectonophysics*, 656, 20–38.

Vannucci, G. and Gasperini, P. (2004). The new re-

lease of the database of earthquake mechanisms of the Mediterranean area (Emma version 2). *Ann. Geophys.*, 47, 307–334.

Vogt, J. (1979). *Les tremblements de terre en France*. Mémoire du BRGM *n*°96. Editions du BRGM, Orléans. 220 p.

Walpersdorf, A., Baize, S., Calais, E., Tregoning, P., and Nocquet, J.-M. (2006). Deformation in the Jura Mountains (France): First results from semi-permanent GPS measurements. *Earth Planet. Sci. Lett.*, 245, 365–372.

Weidenfeller, M. and Zöller, L. (1995). Mittelpleistozane tektonik in einer Lös-Paläoboden-Abfolge am westlichen Rand des Oberrheingraben. *Mainzer Geowissenschaftliche Mitteilungen*, 24, 87–102.

Wiemer, S. and Wyss, M. (2000). Minimum magnitude of completeness in earthquake catalogs: examples from Alaska, the western United States, and Japan. *Bull. Seismol. Soc. Am.*, 90, 859–869.

Wu, P. and Johnston, P. (2000). Can deglaciation trigger earthquakes in N. America? *Geophys. Res. Lett.*, 27, 1323–1326.

Zoback, M. L. (1992). First- and second-order patterns of stress in the lithosphere: The World Stress Map Project. *J. Geophys. Res.*, 97(B8), 11703–11728.